buildings

MDPI

Article

Automated Safety Risk Assessment Framework by Integrating Safety Regulation and 4D BIM-Based Rule Modeling

Dohyeong Kim [1,†], Taehan Yoo [1,†], Si Van-Tien Tran [2], Doyeop Lee [1], Chansik Park [1] and Dongmin Lee [1,*]

[1] School of Architecture & Building Sciences, Chung-Ang University, Seoul 06974, Republic of Korea; rawkasa@cau.ac.kr (D.K.); minsung127@cau.ac.kr (T.Y.); doyeop@cau.ac.kr (D.L.); cpark@cau.ac.kr (C.P.)
[2] Department of Architectural Engineering, Catholic Kwandong University, Gangneung-si 25601, Republic of Korea; tranvantiensi1994@gmail.com
* Correspondence: dmlee@cau.ac.kr
† These authors contributed equally to this work.

Abstract: Performing risk assessments in construction requires collecting and analyzing project data and historical safety accident data, which is challenging due to the inherent complexities and dynamic nature of construction projects. To address these challenges, building information modeling (BIM) has been leveraged as a centralized digital repository that integrates data and provides a holistic 3D view of a project. Previous studies have highlighted BIM's significant functions for risk assessment, such as visualization, simulation, and clash detection. However, these studies often overlook the incorporation of temporal information, which is crucial for assessing risks accounting for the dynamic conditions of construction sites. This study develops a 4D BIM-based risk-assessment framework by integrating spatial and temporal data to respond to dynamic site changes. The framework leverages 4D BIM to combine 3D model data with time-, resource-, and logistics-related information, enhancing the tracking and evaluation of construction progress. The study involves investigating major construction accidents, classifying their risk factors, establishing risk-factor identification algorithms, and implementing the framework on a web-based platform for validation. This approach offers a comprehensive risk-identification strategy, applicable to multiple accident types, with intuitive visualization using BIM models, benefiting from managers' experiential knowledge and enabling effective risk assessments and mitigation strategies. Consequently, potential safety risks at construction sites can be efficiently identified using interconnected spatial and temporal data while tracking changes in risk levels in real time and visualizing them on a web-based platform.

Keywords: safety risk assessment; 4D BIM; rule modeling; spatial–temporal data

Citation: Kim, D.; Yoo, T.; Tran, S.V.-T.; Lee, D.; Park, C.; Lee, D. Automated Safety Risk Assessment Framework by Integrating Safety Regulation and 4D BIM-Based Rule Modeling. *Buildings* **2024**, *14*, 2529. https://doi.org/10.3390/buildings14082529

Academic Editor: Martin Loosemore

Received: 11 July 2024
Revised: 31 July 2024
Accepted: 2 August 2024
Published: 16 August 2024

1. Introduction

In the field of construction, risk assessment is conducted for safety-management purposes to identify potential hazards in advance, evaluate their severity, and establish safety measures [1]. Prompt and accurate risk assessment is a strategic necessity for construction organizations to help them navigate uncertainties, make informed decisions, and remain resilient to critical hazards [2,3]. To perform a risk assessment, project data (e.g., architectural drawings, engineering plans, site location, work schedules, temporary work plans) and historical safety-accident-related data should be collected and analyzed together with related safety regulations. Similar to the efforts of other countries, the South Korean government has increasingly focused on the safety of construction projects, and the Korea Occupational Safety and Health Agency (KOSHA) develops and provides implementation guides primarily based on the severity of risk factors to help construction sites easily conduct risk assessments.

However, collecting and analyzing these data are particularly challenging because of the inherent complexities (e.g., uncertain environment, multiple stakeholders, intricate designs, various materials) and dynamic nature (i.e., changes in scope, design alterations,

unforeseen site conditions) of construction projects. In its efforts to address this challenge, the construction industry has been leveraging building information modeling (BIM) [4].

BIM offers a centralized digital repository that integrates data from various disciplines in real time and provides a holistic 3D view of a project. Several past studies have noted that BIM has many important functions that are useful for risk assessment, such as (1) visualization and simulation [5], (2) clash detection for safety [6], (3) integration with safety standards [7], (4) historical safety-incident data analysis [8], (5) collaboration support for safety communication [9], and (6) safety planning and training [10].

However, despite this promising potential, earlier studies often did not incorporate temporal information, such as construction schedules [11]. Given that construction sites evolve, with new hazards emerging and existing ones changing, it is essential that risk assessments account for these dynamic conditions [10,12,13]. If BIM could be applied to risk-assessment methods that are able to account for dynamic site conditions, it would be possible to prevent and respond to various safety incidents more effectively.

This study was aimed at developing a 4D BIM-based risk-assessment framework by integrating spatial and temporal data to be able to respond to dynamic site changes. Notably, 4D BIM integrates the graphical 3D BIM of the design phase with time, resources, and logistics-related information [14]. One of the benefits of 4D BIM is its ability to track and evaluate on-site construction progress through monitoring and schedule comparisons [15], thereby offering advantages for the planning and monitoring phases of risk management [14]. To develop a 4D BIM-based risk-assessment framework, this study (1) investigated major accidents in construction and their related safety regulations to identify key risk factors; (2) classified discernible risk factors based on 3D model data from 4D BIM and construction schedule information; (3) established algorithms for risk-factor identification using 3D model data, in conjunction with algorithms that can determine task relationships and overlaps based on construction schedules; (4) combined the risk-factor identification algorithms in the correct order to build a risk-identification framework for each accident type; and (5) implemented the 4D BIM-based risk-identification framework on the web, which would allow users to upload models and schedules to visualize daily risk fluctuations.

By utilizing the developed safety risk identification framework, users can expect to obtain risk-identification results that reflect actual construction progress. Through a combination of various risk-factor identification algorithms, a foundation for a comprehensive risk-identification strategy applicable to multiple accident types can be created. Because the results are visualized using a BIM model, they can be conveyed intuitively. Based on the proposed risk-identification framework, it is anticipated that constructing an additional risk hierarchy will not only benefit from the experiential knowledge of managers but also enable risk assessments that offer mitigation strategies.

2. Literature Review

2.1. Traditional Risk-Assessment Methods

Risk assessment requires a procedure for systematically utilizing available information to identify risks and estimate the level of risk for workers [16]. The term "risk assessment" is sometimes used interchangeably with "safety analysis", where the primary objective of risk assessment is to pursue safety through risk elimination and enable the actual removal of specific risk causes without disrupting or altering the system [17]. Risk assessment is performed to evaluate operational risks, typically providing a hierarchical representation of possible events, following a procedure to estimate and calculate the likelihood and severity of potential outcomes of specific events or combinations of events [16,18,19].

Various risk-assessment methods have been applied to different industrial processes [6,20]. Traditionally, checklists have been widely used in construction, but they tend to cover only predetermined risks and may overlook less obvious or emerging risks [21,22]. On the other hand, techniques such as job safety analysis (JSA), risk matrices, fault tree analysis (FTA), dynamic risk assessment (DRA), and safety culture

assessment have also been used for risk assessment at construction sites [12,23–25]. However, there are several challenges with construction risk assessment due to a number of factors, as follows. First, construction projects often involve numerous stakeholders, intricate processes, and changing hazards, making it difficult to identify and evaluate all risks comprehensively. Second, construction environments are inherently unpredictable, with changing conditions, unforeseen events, and evolving regulations, making it challenging to anticipate and mitigate risks effectively. Third, risks in construction are often interconnected, meaning that addressing one risk may impact others, thus requiring a holistic approach to risk assessment and management. Fourth, limited or unreliable data, inadequate documentation, and incomplete information regarding site conditions or project specifications can hinder accurate risk assessment. Fifth, construction involves human labor and decision-making, which introduce the potential for errors, miscommunications, and unequal levels of expertise, further complicating risk-assessment efforts [8,26–28]. Therefore, a powerful platform for improving risk assessment in construction that enables better data integration, visualization, collaboration, and analysis throughout the project lifecycle is essential. This enhanced capability may help construction teams identify, analyze, and mitigate risks more effectively, ultimately leading to improved project outcomes and reduced project risks.

2.2. Necessity for 4D BIM for Risk Assessment

BIM provides an intuitive site plan and effective linkage of risk-related information to BIM modeling elements, facilitating early risk identification, risk-averse planning [4,29], and the visualization of work targets according to construction plans [30]. Given these potential benefits, BIM has been researched for the development of safety tools that can identify potential construction risks during the design phase. For example, BIM models can identify and visualize risks through simulations interfaced with the models [31] and detect potential conflicts by incorporating construction-planning information to discern construction-related risks [5]. The concept of rule-based risk identification also enables automatic computation of the risk levels of each individual work unit by extracting geometric data from BIM model elements [11,32]. Additionally, the integration of BIM with knowledge-based systems to identify risks using geometric data based on safety regulations has been proposed [4,32,33]. A number of research studies have combined BIM and related databases to incorporate the concepts of prevention through design to provide risk identification and solutions to users [34–36].

Several attempts have, therefore, been made to integrate scheduling with 3D BIM to form what is known as 4D BIM, considered to be a single step from the traditional concept of BIM. Four-dimensional BIM consolidates spatial and temporal data, making it a viable concept for dynamic site analysis, safety analysis, evacuation planning, and construction progress monitoring [8,26,27]. Four-dimensional BIM not only incorporates graphic-based spatial data generated during the design phase but also adds information related to time, resources, and logistics [14]. This enables the transmission of extractable information, identifying the worksite, activity timing, and objects, for specific purposes to construction personnel [27]. Furthermore, 4D BIM provides the advantage of tracking and evaluating construction progress within a construction site through schedule comparison, thereby facilitating effective project planning and monitoring [15]. The benefits of 4D BIM have been covered extensively by earlier studies [28,37].

However, only a few research studies have focused on comprehensively assessing safety risks using 4D BIM [38]. While some investigations have utilized BIM data for risk identification according to certain rules or specific algorithms, it has been typical for a single study to focus on identifying risks for only a single type of accident or a single task based on an algorithm customized only for a specific task, thus revealing inadequacies in providing a comprehensive safety-management strategy [11,32,34–36]. In addition, the complexity of using BIM-based risk-assessment tools poses a challenge to industry adoption [15,39]. Manual risk assessments can be time-consuming and prone to errors

and cannot ensure consistency across projects and teams. Although a number of studies have automatically identified potential safety concerns, responses to these concerns were applied solely during the design phase [12,40] and thus did not reflect risk-level changes that occur as construction progresses.

Upon a meticulous review of past research, it becomes apparent that traditional risk-assessment methods have limitations in resolving challenges stemming from the dynamic nature of construction projects. Despite the potential of BIM as a risk-assessment tool, it has remained limited with regard to providing comprehensive assessments and failed to address usability challenges. Similar limitations have also been observed for studies utilizing 4D BIM integrated with scheduling information, thus necessitating a comprehensive risk-assessment strategy capable of reflecting site variability. Therefore, this study aims to present a starting point for a dynamic risk-assessment method centered on risk identification, which is the initial step in risk assessment, based on 4D BIM. It is essential to develop a framework that enables the identification of risks pertaining to various types of accidents, rather than being limited to assessments based on a single accident category.

3. Materials and Methods

This study proposes an automated safety-risk identification framework that employs 4D BIM to integrate spatial and temporal information to enable the tracking and monitoring of changes in working conditions on a construction site as the project progresses and be able to respond to corresponding shifts in risk levels. This framework is constructed on a web-based platform, where 3D models and work schedules are integrated to establish a 4D BIM environment and where the framework can be directly validated. This section presents an overview of the framework and the classification of the risk-factor information necessary for comprehensive risk assessment.

Figure 1 illustrates the research method used in this study. First, the risk factors are classified based on two key data sources: 3D models and work schedules. These sources are chosen to discern risk factors containing both spatial and temporal information. Afterward, various accident statistics and real case studies are analyzed to create scenarios. For each scenario, a method is devised to determine the risk factors that should be proactively identified and how to combine these factors. This scenario-based approach is adopted to enhance the practicality and applicability of the framework to real-world construction sites. Subsequently, risk-factor identification algorithms are developed to identify risk factors based on spatial information from 3D models and temporal information from work schedules. Finally, the risk-identification framework is constructed on a web-based platform. This platform allows 3D models and work schedules to be uploaded, which are then incorporated into the developed algorithms to identify risks. The proposed framework is then validated using the implementation platform to verify its applicability and reliability.

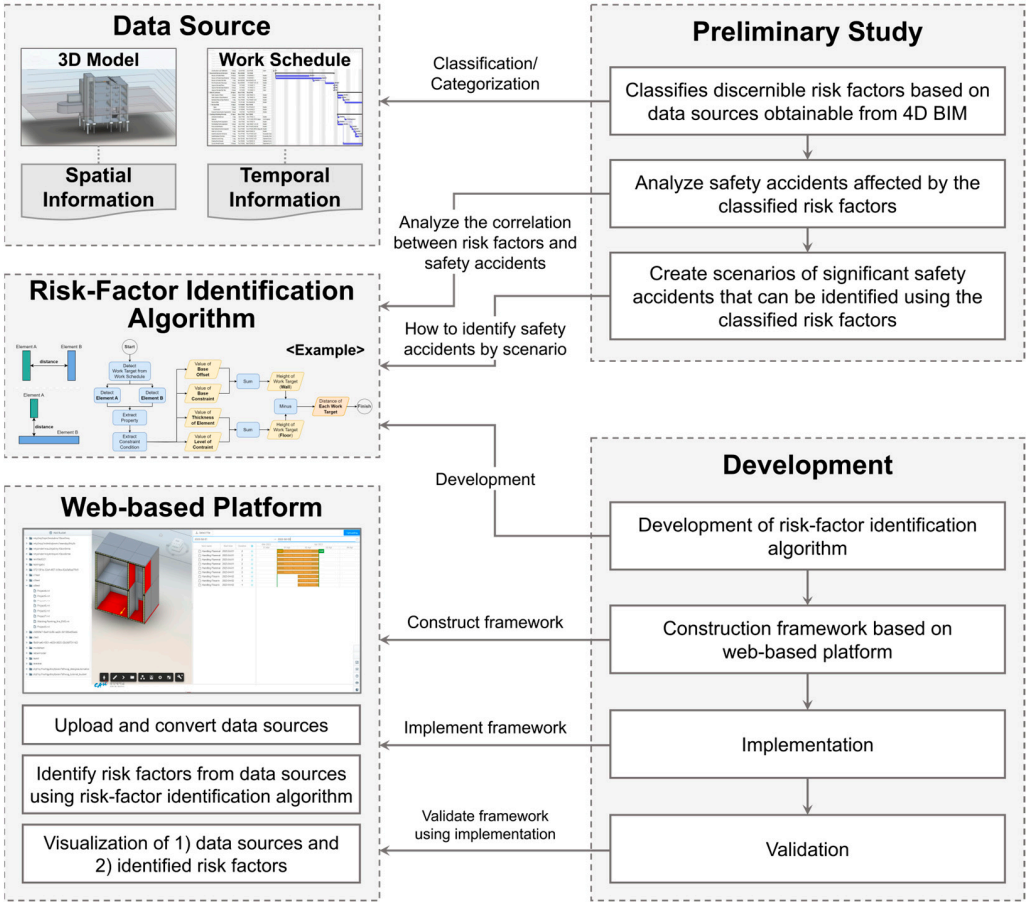

Figure 1. Research method.

3.1. Risk-Factor Classification Based on 4D BIM Data Sources

This section reclassifies risk factors based on those analyzed in past studies. Prior to this, we identify the types of data available to the 3D model and task schedule and the two data sources included in the 4D BIM-based risk-identification framework.

Four-dimensional BIM integrates 3D graphical design information from the design phase with temporal information, such as construction-planning data, and offers a comprehensive model-based approach [41]. The 3D model encapsulates all attribute data for individual components, while the work schedule details the time, resources, and logistics. To construct the risk-identification process, the 4D BIM data are first categorized based on the two main sources: the 3D model and the work schedule. The 3D model incorporates data on building components, such as materials, size, exterior and interior layouts, and geometric data. Hence, through the use of specific algorithms or application programming interfaces (APIs), these data can be acquired to determine the spatial information useful for risk identification, such as the work target height or the distances between targets. On the other hand, the work schedule offers temporal data, including task sequences, durations, names, and subjects, allowing dependencies between tasks to be ascertained and potential concurrent risks to be identified. Based on the data obtainable from 4D BIM, discernible risk factors are reviewed, and, based on a comparison with risk factors analyzed in past research, those viable for the 4D BIM-based risk-identification framework are reclassified.

To construct the risk-factor identification algorithm, an analysis of the risk factors is conducted. During the operation of the framework, risk factors are analyzed and classified based on required information, with some references to earlier studies. In construction-related research, risk factors refer to those that affect risk in construction projects. However, this study requires an analysis of the risk factors that contribute to the occurrence of safety accidents at construction sites. According to statistics, approximately 80% of safety ac-

cidents occur owing to the unsafe behavior of workers, and thus, our review includes a number of risk-factor classification studies that specifically analyzed the effect of worker behavior [42,43]. Meng et al. analyzed the risk factors influencing the occurrence of accidents, addressing not only the unsafe behavior of workers but also the correlations of factors related to construction safety accidents [44]. Whereas earlier studies have categorized risk factors into organizational, safety, cultural, and personal factors, Meng et al. further refined the classification into individual, organizational management, project, and production operation levels [44,45]. Table 1 presents the classification of risk factors for safety accidents identified in past studies.

Table 1. Classification of risk factors.

Level	Details		Research
Individual	Physical factors	Musculoskeletal disorders Physical fatigue	[45,46]
	Psychological factors	Emotions Stress Personality Cultural, regional differences	[47–55]
Organizational Management	Organizational	Safety culture Work norms	[56–60]
	Managerial	Manager's behavior Managerial leadership	[61,62]
Project	Safety investment Safety inspection feedback Interactions between organizations and managers		[63–65]
Production/ Operation	Work methods		[66–70]
	Work environment	Weather Work location	
	Resources	Construction equipment Construction machinery Materials	

Following the procedure, the project manager conducts the risk assessment based on pre-prepared work-related information, such as work plans, which typically include resources, equipment, machinery, project drawings, and construction-planning dates. Most of these data are prepared before on-site construction begins. However, whereas past research studies have identified risk factors such as individuals, organizational management, and influencing factors in their analyses, these factors are generally not included among the information held at construction sites. Thus, from this examination, it is apparent that additional analysis and research are necessary.

In this study, several algorithms that automatically extract schedule-related spatial and temporal information from 3D models and work schedules, relevant to identifying the risks, are developed. Based on these data sources, the risk factors are reclassified to serve as origins of information. This classification process is based on the individual characteristics and data sources for each risk factor. Specifically, the criteria for selecting and classifying risk factors are (1) not requiring separate analytical tools and (2) basing information sources on pre-existing materials at the construction site (e.g., 3D models and work schedules). These factors are further classified under safety regulations, work conditions, work environment, construction equipment, and machinery. Initially, the risk factors are classified based on their characteristics according to data sources used to construct the risk-factor identification algorithm. Subsequently, a separate combination method is defined to utilize each identification algorithm in the framework, and with these algorithms, the types of risk factors are selected and classified.

3.1.1. Classification of Risk-Factor Characteristics Based on Data Source

- Spatial Characteristics: Unique characteristics of space, which include physical attributes, such as confinement, distance, and height, pertaining to the area or object of the work.
- Operational Characteristics: Unique features of the input resources required for task execution, such as materials, substances, and machinery or equipment.
- Temporal Characteristics: Unique features concerning the timing of task execution, including the duration and time frame based on the work plan.

Following this classification, the risk factors are sorted into spatial, operational, and temporal characteristics. Each characteristic is distinct and nonoverlapping and can be viewed in terms of the source of information. Based on the characteristics of the classified risk factors, spatial attributes can be acquired from 3D models based on spatial data, whereas risk factors with operational and temporal characteristics can be obtained from the work schedule.

3.1.2. Classification of Risk-Factor Types of Combination Algorithms

In construction safety, risk factors that influence the occurrence of accidents can exist independently, causing accidents on their own, or can interact under the concept of multiple causality, where several factors jointly contribute to an accident. Moreover, on a construction site, variability in working conditions can arise as a result of specific tasks or objects, leading to the potential for the sporadic emergence of risk factors, either present or absent. To address this, risk factors that influence accident rates are classified into three types that enable the application of the multiple-causality concept to risk identification to elucidate their interrelations. This causal relationship is later used to determine the presence or absence of risk based on a combination of specific risk factors during the final risk-identification process. In this classification, the risk factors are classified into "Independent", "Combinatory", and "Mitigatory" risk factors. Incorporating these types into risk identification allows for the recognition of risk reflective of the variability at construction sites.

- Independent Risk Factors: Indicate a high accident likelihood and severity based on a single material, substance, machine, target object, or characteristic. Confined spaces are a well-known example of this type of risk factor; such spaces are associated with a high safety risk owing to the potential presence of toxic gases or a lack of oxygen. Thus, safety regulations from organizations such as KOSHA in South Korea and the Occupational Safety and Health Administration (OSHA) in the United States underscore the need to pay attention to such factors.
- Combinatory Risk Factors: Individually may not present a high likelihood or severity of accidents but become significant when combined with other factors. Examples include open flames, flammable materials, concurrent operations, and shared workspaces. For instance, whereas open flames alone in a work schedule may not imply high risk, if combined with flammable materials, concurrent operations, and a shared workspace in proximity, the risk of fire accidents escalates significantly.
- Mitigatory Risk Factors: Reduce risks; examples include executing specific safety-improvement tasks or installing safety equipment. Activities such as sealing work-created openings can also be categorized under this type of factor, although these are not intended primarily for safety. However, under the concept of multiple causality, these factors sometimes increase risk in certain contexts, highlighting their nuanced role in risk management.

These risk factors can overlap depending on the working conditions and vary based on the diverse characteristics of sites, work types, and project specifics, leading to different types of accidents or variabilities. The criteria for classifying risk factors, i.e., the characteristics and types, serve distinct purposes. The characteristics aim to identify the source

of data for risk-factor information, whereas the types combine risk factors for the final identification of risks.

3.2. Accident-Type-Based Scenario

In the preliminary phase, risk factors that affect the potential for construction safety accidents are categorized based on data sources of spatial and temporal information. Whereas developing respective identification algorithms for these factors is essential, it is also crucial to determine the algorithms to be applied for each type of accident. Rather than formulating an algorithm for a specific accident type, this study aims to combine various risk-factor identification algorithms to cater to a diverse range of accident types. Consequently, based on an analysis of construction-site accident statistics and cases, scenarios involving predominant accident types are constructed. Additionally, relevant safety regulations are reviewed to understand the risk-factor information essential for risk identification in these scenarios.

The data used to select the accident types include accident statistics, actual accident cases, and safety regulations published by various institutions, such as KOSHA, OSHA, the Center for Construction Research and Training (CPWR), and the Bureau of Labor Statistics (BLS). Given the variability in the types of construction sites, quantifying the intensity and frequency of each accident type at construction sites may be challenging. However, based on statistical data, it is feasible to gauge the general accident types and their corresponding intensities and frequencies. Among these, those that either commonly occur or are perceived to have a high intensity when they do occur are selected. These selected accident types include falls, struck-by injuries due to vehicular accidents, exposure to harmful substances or environments, hits by falling objects, fires and explosions, and musculoskeletal disorders from repetitive motions. Musculoskeletal disorders, which are a type of injury or disease, are included to consider factors that could potentially lead to safety accidents. Table 2 highlights a variety of accident types, their statistics, descriptions, and significance based on data from agencies such as OSHA, BLS, CPWR, and the National Institute for Occupational Safety and Health (NIOSH).

Table 2. Summary of key accident types in the construction industry recorded in the United States.

Accident Type	Description	Severity
Falls	Falls from elevated areas (scaffolding, ladders) to lower levels and structural collapses.	379 fatalities in 2021 [71]
Struck-by	Inadequate work-zone control, absence of signalers, vehicular equipment accidents (40% of collision accidents).	150 fatalities in 2021 [72]
Exposure to harmful substances or environments	Poor ventilation in enclosed spaces; exposure to hazardous gases and smoke.	205 fatalities in 2021 [73]
Hits by falling objects	Insufficient control of risk areas, not wearing safety helmets, adverse weather conditions.	90 fatalities in 2019 [74]
Fires and explosions	Inadequate management of flammable materials; neglect in installing spark-proof nets during flame operations.	9 fatalities in 2020 [75]
Musculoskeletal disorders	Repetitive motions, prolonged work in uncomfortable postures.	Over 20% of nonfatal injuries [76]

To validate the applicability of the risk-identification process proposed in this study, test scenarios were prepared based on an analysis of accident cases of various accident types. Through analysis and scenario creation, the patterns of accident occurrence and risk factors were then identified. Based on the findings, preventive measures and related safety regulations were referenced and applied to the configuration of the risk-identification process.

Table 3 provides a comprehensive overview of the different accident types, their specific cases, and the recommended safety regulations. It is essential to understand the

nuances of each accident type to ensure the effectiveness of the proposed risk-identification process.

Table 3. Summary of accident cases, safety regulation keywords, and scenarios by accident type.

Falls and Collapse	Accident Case	The occurrence of collapse and fall accidents during work without a safety inspection after the installation of scaffolding on a sloped section.
	Scenario	(Slope) A scenario of scaffolding installation on a slope with upper wall and ceiling work scheduled on the scaffolding. (Step difference) A scenario with a step difference in the work area and planned work using a mobile work platform.
	Safety Regulations	Structural defect precautions, prior measures, expert scaffolding advice, scaffold fastener installation, scaffold toppling prevention.
Falls	Accident Case	During material cleanup, a worker fell from a height of 4.5 m (15 ft) through an 80 cm (2.6 ft) gap onto a concrete floor.
	Scenario	In construction, situations where the inner diameter of the pre-tensioned spun high-strength concrete (PHC) pile used is more than 80 cm.
	Safety Regulations	Installation of safety railings and covers, marking of installed covers, caution with cover materials, and immediate restoration after necessary dismantling work.
Hits by Falling Objects	Accident Case	A worker installing exterior panels on a roof accidentally dropped one, which struck another worker 7.5 m (24.6 ft) below, resulting in death.
	Scenario	Exterior wall finishing work using autoclaved lightweight concrete (ALC) bricks, with landscaping work planned in the lower area.
	Safety Regulations	Implement mandatory safety measures in areas at risk of falling objects, avoid simultaneous top–bottom work, designate and restrict access to hazardous areas, and wear safety helmets.
Fires	Accident Case	Fire incidents in the UK (2014) and Texas, USA (2017), due to sparks from welding operations coming into contact with flammable materials nearby.
	Scenario	Welding operations planned within an elevator pit, with simultaneous epoxy painting operations using epoxy paint planned in the adjacent basement area.
	Safety Regulations	A preliminary survey of nearby inflammable materials before welding, the appointment of fire watchers, spark prevention measures, and emergency equipment readiness.
Suffocation	Accident Case	Suffocation incidents in India (2018) due to toxic gases such as hydrogen sulfide in confined spaces, and another in South Korea (2019).
	Scenario	Painting work in a basement machine room using epoxy paint, followed by additional finishing work.
	Safety Regulations	Caution with synthetic materials, ventilation, mandatory entry-permit procedures, confined space awareness, entry permits valid for a maximum of 8 h, and appropriate measures required for additional work.
Struck-by Injuries	Accident Case	A worker cleaning behind an excavator was struck and killed by the excavator as it reversed.
	Scenario	Excavation work using an excavator, with other work planned in the vicinity.
	Safety Regulations	Understand the excavator's turning radius, have a mandatory safety plan for excavation work, recognize any workers/obstacles in the working radius before starting, park on flat ground, implement measures to prevent tipping, and conduct mandatory signaling work.
Musculo-skeletal Disorders	Accident Case	Risk of acute and chronic back pain due to prolonged work in uncomfortable postures. Increased risk of suffering a herniated disc when working outdoors in cold temperatures.
	Scenario	Ceiling work requires a high-altitude work platform, but conditions necessitate the use of a Type A ladder, with continuous work planned for three days.
	Safety Regulations	Recommendation to use scaffolding for work above ~3 m (10 ft), limited time working on a ladder, caution with prolonged high-altitude work, and recommended appropriate rest periods.

3.3. Combination of Risk-Identification Algorithms for Different Scenarios and Application of Risk-Identification Framework

Slip/Fall/Step Difference/Mobile Platform: This scenario involves the use of mobile platforms, such as mobile scaffolds, in areas with floor elevation differences for tasks performed on ceilings. It is crucial to monitor fall-related risk factors due to these floor variances. Initial evaluations should ascertain the use of the phrase "mobile platform" in the work plan. Afterward, the region in and objects on and around which the mobile platform will operate should be assessed to detect any elevation discrepancies. If such irregularities are detected, workers should be promptly made aware of them. The floor peculiarities in such work zones bear similarities to those in the subsequent scenarios involving slopes.

Fall/Collapse/Slope/Scaffolding: This scenario involves the erection of scaffolding on an inclined region planned for ceiling work, necessitating operations on top of the scaffolding. It is crucial to monitor the risk factors related to potential scaffolding collapse and ensuing fall incidents. First, the inclusion of the phrase "work atop a scaffolding" in the work plan should be verified. Then, past construction records should be analyzed to confirm that the region of scaffolding installation is a "slope". Subsequent evaluations should ascertain whether a "safety check" has been scheduled before commencing work on scaffolding on the slope. If the scaffolding is located on an "incline", it is essential to determine whether a planned "safety check" is in place before work initiation. If no safety checks are planned, there is a need to integrate plans for structural safety assessments before the task can be started. Through adherence to this procedure, it becomes feasible to identify and implement preventive measures and effectively manage the risks associated with working on scaffolds positioned on slopes.

Hit by Falling Object/Outer Wall: This scenario involves materials or tools that may fall from a height and hit workers below. The assessment begins with checking the work schedule for the phrase "outer wall tasks". It is then determined whether there are any jobs located "above 2 m" and, if yes, whether the materials pose a falling risk. If this is the case, it is essential to check for planned tasks that are scheduled to be carried out simultaneously in the upper and lower sections. Lastly, the "simultaneous planning" of tasks is verified. Applying this risk-identification process helps identify potential risks related to falling-object hazards, based on which the information about controlled zones can be visually conveyed.

Fire/Firearm/Flammable Material/Space Connection: This scenario involves planned welding tasks that will be carried out in an elevator pit and will coincide with scheduled epoxy-resin-coating tasks to be carried out in the basement below. Initially, the work schedule is checked for the phrases "fire-handling tasks" and "flammable-material-handling tasks". It is then determined whether these tasks are "simultaneously scheduled". If the work zones are not interconnected, the risk of welding sparks reaching and igniting the flammable materials is low. To confirm this, the "spatial connection of work zones" is assessed by evaluating the distances between the work zones. Safety regulations specify horizontal and vertical distances of 11 m from welding tasks that generate sparks. When these factors are properly considered and the appropriate risk-identification algorithm is applied, potential fire hazards can be identified, particularly focusing on "fire-handling tasks" and "flammable-material-handling tasks" that could be potential sources of ignition.

Suffocation/Toxic Gas/Enclosed Space/Ventilation: This scenario involves the use of epoxy paint, which generates toxic gas, in a machine room with only one door, which makes ventilation challenging and increases the risk of suffocation. It is essential to first determine whether a "confined space" exists within the workplace. Confined spaces can easily lead to dangerous situations; therefore, further assessment of additional risks is necessary. Accordingly, the type of work performed within confined spaces should be identified, followed by an evaluation of whether "artificial materials" or "toxic gases" are being used. The work schedule is then reviewed to check whether "ventilation" has been planned and to ensure adequate air circulation. If appropriate measures such as ventilation

checks or toxic-gas checks are not planned, and "additional tasks" proceed without these measures, the risk of suffocation accidents increases.

Musculoskeletal Disorders/Repetitive Work/A-Type Ladder: This scenario involves a planned ceiling task that requires the use of an A-type ladder for three days, which would likely result in a significant daily workload. Given the use of an A-type ladder for this ceiling work, this task will involve working in uncomfortable positions, which increases the potential for musculoskeletal disorders. To avoid these risks, OSHA recommends using scaffolds for tasks performed at over ~3 m (10 ft) high. If the use of scaffolds is not feasible, partial ladder use is permitted. Additionally, minimizing the work duration on ladders is highly helpful for reducing these risks. The first step in identifying the risk of musculoskeletal disorders is to verify the inclusion of ceiling tasks in the work schedule. From this, it is necessary to determine whether the target of the task is located "above 10 feet" and confirm the use of ladders instead of scaffolding. The work schedule should also be reviewed to determine whether prolonged tasks are planned to determine whether there are any daily work durations that would exceed 8 h. Finally, for tasks that use an A-type ladder, it is essential to ensure that more than two workers are assigned. In this study, only the work schedule and BIM model are considered; the number of workers deployed is omitted.

3.4. Construction of Algorithms for Individual Risk-Factor Identification

The meticulous execution of construction operations necessitates an understanding of the various risk factors that could potentially interfere with the workflow or compromise the safety of workers. Recognizing these risk factors and constructing suitable algorithms to detect them automatically are essential for proactive risk management. This section elaborates on the algorithms designed to discern specific risk factors based on spatial, temporal, and work-related characteristics.

Figure 2 depicts an algorithm designed to gauge the distance between two areas of operation by comparing the heights of the work targets.

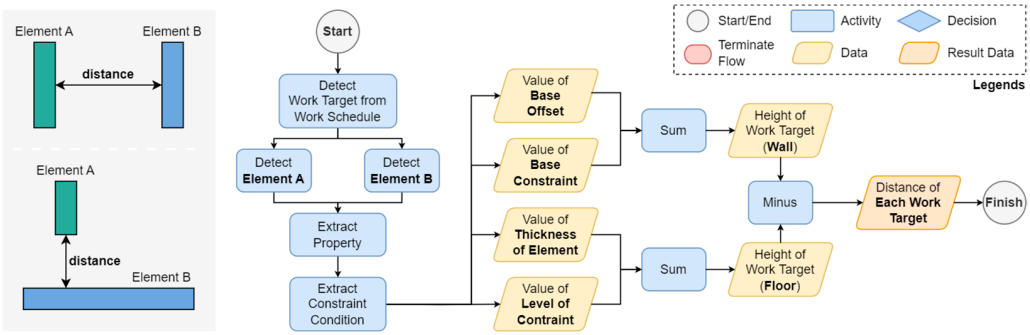

Figure 2. Algorithm for determining distance between work elements.

Figure 3 outlines an algorithm for determining whether a specific work area is enclosed. In Autodesk Revit, the "Room Tag" feature, which designates rooms and visually represents their information and attributes, such as name, area, volume, and number, is also useful for determining whether a space is enclosed. While not all spaces with a Room Tag are enclosed, some, such as boilers or machine rooms, can be considered enclosed if they are surrounded by walls. Additionally, geometric data can be used to assess whether a space is confined. Reviewing the form of the room walls and their connectivity to the floor slabs can provide insights into the enclosure status of the room. For example, if the walls are interconnected, the room can be viewed as an enclosed space. Entrances and exits that are vital for ventilation must be considered. However, if a room is located underground or has limited access points, it may lack ventilation; thus, it is deemed an enclosed space.

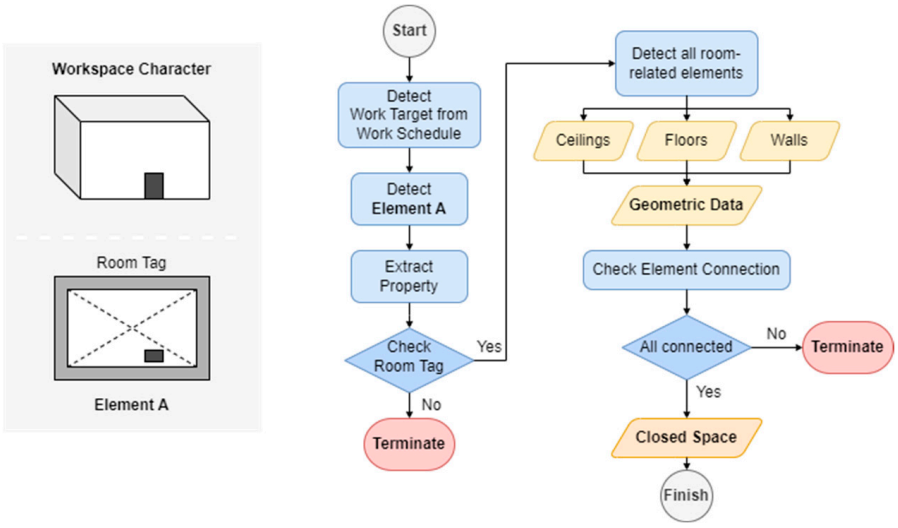

Figure 3. Algorithm for determining enclosed workspaces.

Figure 4 shows an algorithm for discerning differences in floor level or height. Although Revit does not directly offer a feature to detect floor irregularities, it allows access to data on the levels, floors, and constraints of modeled elements. Through comparisons of the floor heights of floor-slab elements modeled at the same level, floor inconsistencies and steps can be identified. However, it is vital to note that some floor irregularities might be undiscernible in BIM models owing to the real-world characteristics of construction sites.

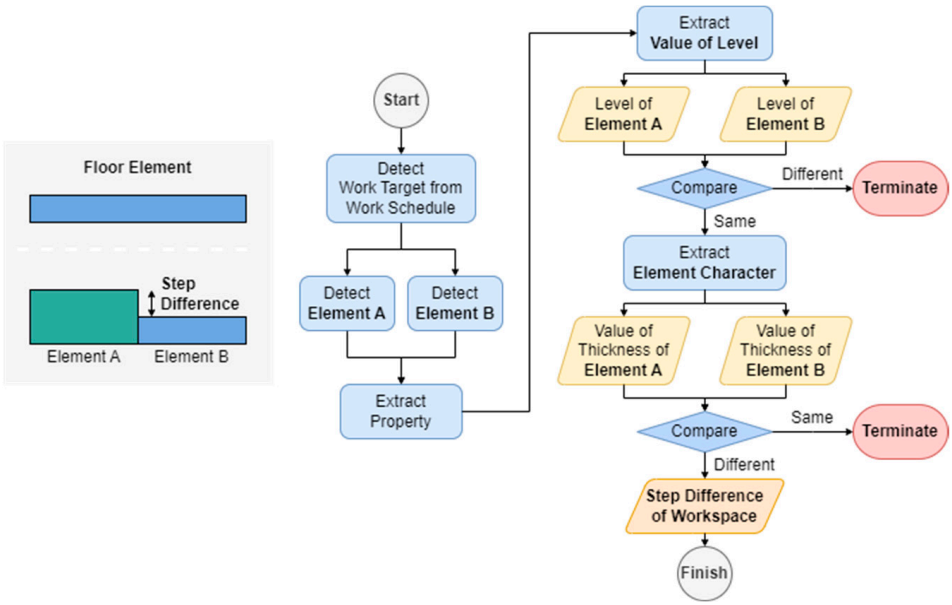

Figure 4. Algorithm for determining floor-level differences or heights.

Figure 5 shows an algorithm for detecting the presence of a slope. Revit includes features for modeling and defining slopes. Identifying the level and slope elements can reveal whether a slope exists in a scenario. Moreover, a slope creates a gradient on a floor surface, and based on its properties, the presence and characteristics of the slope can be assessed.

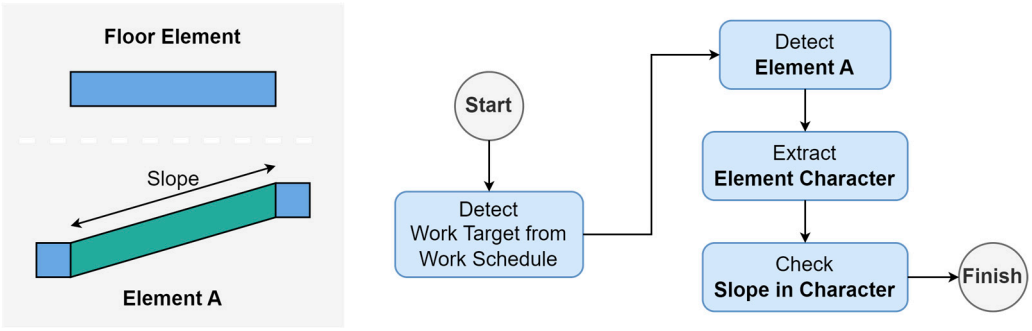

Figure 5. Algorithm for determining existence of slope.

Figure 6 shows an algorithm for determining material characteristics based on 3D model components. Revit provides features for modeling elements that reflect object characteristics, allowing the characteristics of an element to be obtained. Based on the properties included in each element, desired information, such as the shape or material, can then be derived, allowing risk identification to be performed for the material. However, to determine risks based on this information, the elements need to have been accurately modeled in the first place.

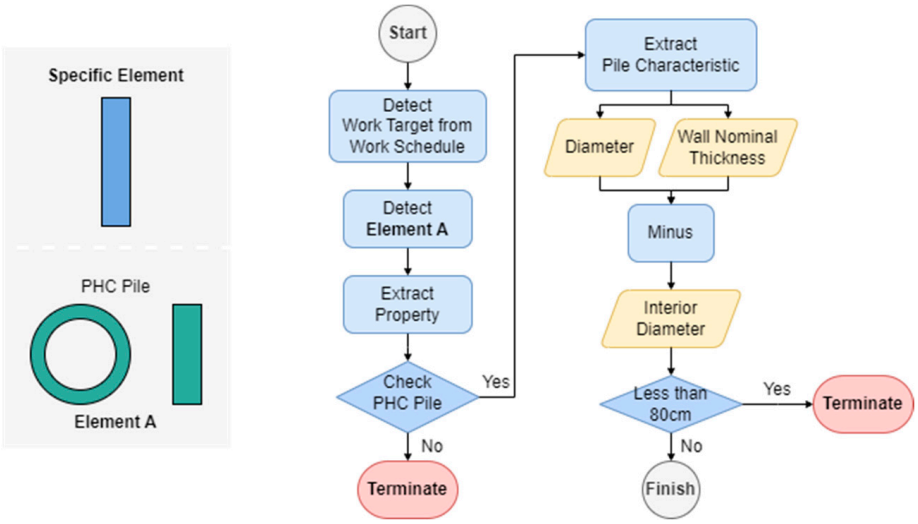

Figure 6. Algorithm for determining input material characteristics.

Figure 7 illustrates a risk-factor identification algorithm based on work schedules, which assesses risks according to task precedence and construction progress. Because construction operations are interconnected, understanding the entire workflow is essential for efficient risk management. For instance, if a risk is identified in a specific work unit, it is essential to review the work plan to determine whether preventive measures should be executed before or after that work, because risk levels change as construction progresses. For example, adequate ventilation is required during or after tasks involving toxic substances in enclosed spaces. Safety regulations also recommend avoiding concurrent tasks in the same or adjacent areas. Therefore, different adjacent work areas should be checked to see whether they are scheduled simultaneously and whether any overlaps exist. Finally, sequences comprising a specific task that generates a risk factor and a subsequent task that naturally mitigates it should be identified.

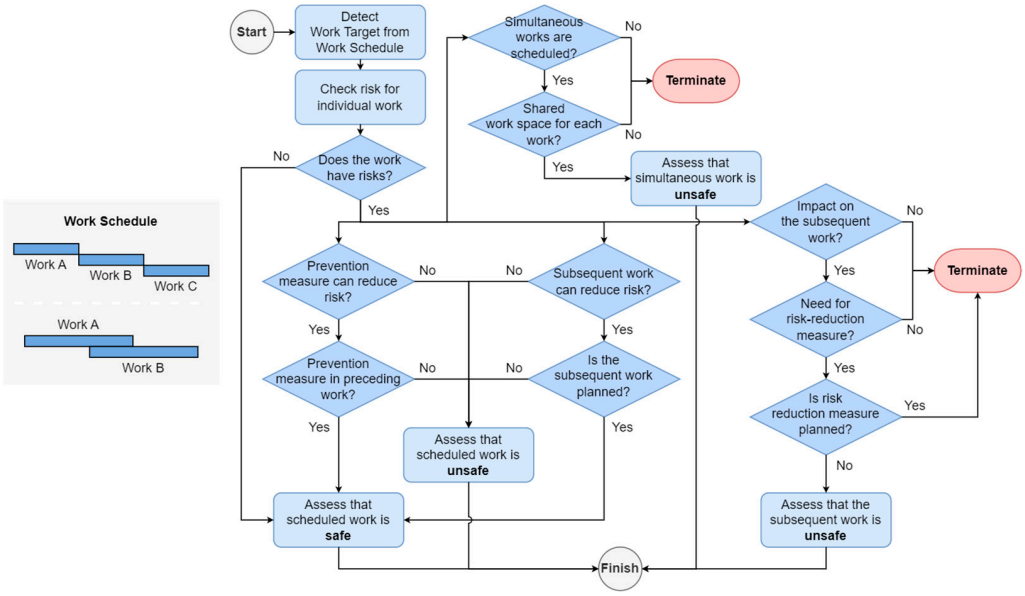

Figure 7. Algorithm for determining effects of construction-task schedules.

Every modeled element possesses a unique ID that is used to match the element with its corresponding schedule data, determine the timing of operations, and extract specific properties. However, unlike other elements, openings in a 3D BIM model do not have unique IDs. Instead, they assume the unique IDs of all elements to which they are connected. Consequently, the different connected openings share the same unique IDs.

For example, in Figure 8, we can identify 11 wall elements (W01–W11), five floor elements (F01–F05), three vertical openings (A, B, and C), and one horizontal opening (labeled D). Vertical opening C assumes the unique IDs of adjacent elements F01 to F04. Vertical opening B takes on the IDs of its neighboring elements F03, W04, and W05. Vertical opening A, which is adjacent to horizontal opening D, shares IDs F04, F05, and W06, meaning that both A and D are assigned the same IDs.

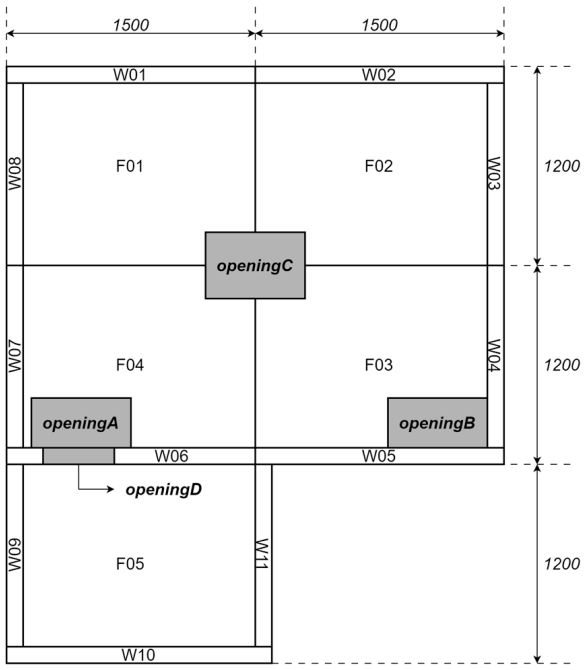

Figure 8. Example of openings in design.

Elements such as doors and windows are uniformly treated as horizontal openings. If a door is installed on a wall, its Material ID matches that of the installed wall. Because most horizontal openings, such as doors, are typically adjacent to floor elements, the Material IDs of the door will include those of the wall and floor. If a vertical opening, such as an elevator pit, is installed on only one floor, its Material ID is set to be the same as that of the floor on which it is installed. However, if the vertical opening is adjacent to other floor elements, then its Material IDs will contain the IDs of those floors.

3.5. Development of 4D BIM-Based Risk-Identification Framework

The risk-identification framework proposed in this study comprises two primary modules:

- Risk Identification Module (RIM): This module focuses on the risk-factor identification algorithm and the risk-identification process formulated based on this algorithm. By leveraging a unique ID, the RIM integrates the 3D model with the work schedule, thereby enabling effective risk identification.
- Visualization Module (VM): This module utilizes the visual advantages of BIM by incorporating a simulation feature that allows visual inspection of the 3D model. Through integration with the work schedule, it introduces a date-selection feature, with which the risk-identification results can be reviewed, and a corresponding work-schedule upload function. Moreover, the VM includes a feature for displaying the work schedule, which can help identify tasks that cause the identified risks. The essence of this module is a function that intuitively conveys the risk-identification results by highlighting the relevant work targets.

The framework operates sequentially: the RIM is activated first, followed by the VM. First, a 3D model of the target construction project and its associated work schedule are uploaded. Once uploaded, the RIM performs risk identification and generates results. Subsequently, once the desired date is selected from the work schedule, the risk-identification results are visualized on the 3D model.

Figure 9 illustrates the methodology that structures the risk-assessment process. The configuration of this process combines the identification algorithms in sequence based on specific accident risk types or scenarios. Each deployed algorithm operates sequentially, acquires data selectively, and synthesizes them to generate the necessary information. In other words, the risk-assessment process is structured by internally integrating the identification algorithms according to the accident scenarios.

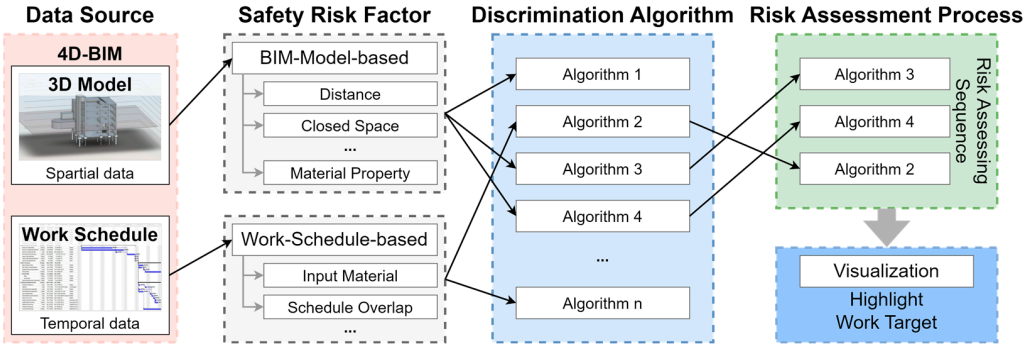

Figure 9. Construction and configuration of risk-factor identification and assessment process.

Although the type of accident remains consistent across scenarios, the identification methods and the sequence of algorithm application can vary based on the working conditions. This section describes the construction of the risk-assessment process for each scenario based on the risk-factor identification algorithms formulated in Section 3.2.

3.6. Implementation of Proposed Framework on BIM Platform

Figure 10 depicts the system architecture of the prototype implementation of the proposed framework. For this implementation, Autodesk Forge was selected as the foundation for building the prototype system because it provides several APIs that are useful for leveraging and maximizing the benefits of 4D BIM in terms of accessibility, visualization, and information sharing using JavaScript, a widely used programming language that enables the dynamic creation and control of content and multimedia. Autodesk Forge was used to implement the server, which contained the key functions proposed in the framework. These functions were constructed based on the available APIs, which are managed by the Autodesk Forge Bucket (Figures A1 and A2). These functions can be categorized into three types: (1) information retrieval, (2) information analysis, and (3) information delivery.

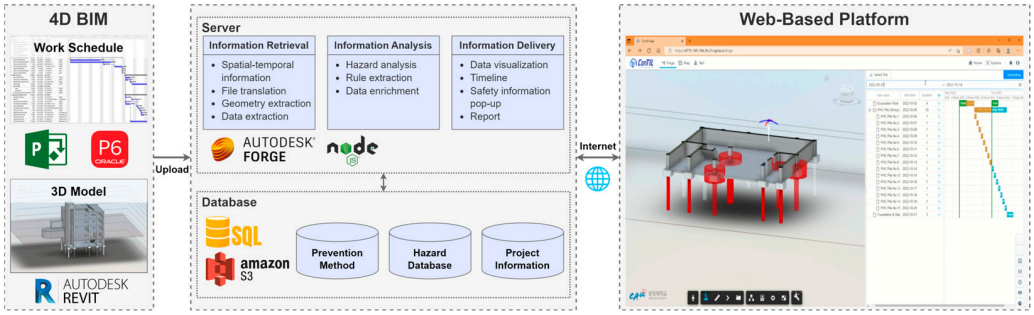

Figure 10. System architecture of prototype implementation.

These functions are initiated by the upload of data sources: specifically, BIM models and schedules. Because the web-based platform was developed using Autodesk Forge, the prototype system focused on utilizing 3D models created using Revit, which is also serviced by Autodesk and uses the file type RVT. Hence, the capability to upload RVT files onto the web platform was established (Figure A3). The uploaded RVT files are then converted into web-compatible 3D models (Figures A4 and A5).

Simultaneously, a function for uploading work-schedule files was established. Because documents such as work schedules and progress charts are commonly developed using Microsoft Excel and Oracle Primavera P6, this function was designed to accommodate the universally adopted Excel file format and ensure compatibility with Primavera P6. When a work schedule is uploaded to the platform, it is converted into a Gantt chart format for effective visualization and management within the web-based platform.

Subsequently, to operationalize the purpose of the framework, which is system-risk identification, the uploaded work-schedule data are retrieved and integrated with the 3D model. When a work schedule is uploaded, key information such as task names, materials used, and specific material safety data sheet (MSDS) numbers are extracted, together with temporal data such as work hours (Figure A6). This allows for a synchronized representation of construction progress and associated risks via the acquisition and selection of work dates, enabling the algorithm to analyze and overlay the temporal project data with the spatial model data. Furthermore, tasks and their target elements are matched by fetching the required information from the 3D models, work schedules, and the IDs assigned to each work target element.

After the retrieval of data sources and their interconnections, the prototype system must analyze them to provide essential feature-risk identification. Table 4 shows the specific formulas and particulars regarding work schedules and element characteristics used within the APIs in the Bucket. Item 1 presents a formula that determines the construction progress based on the work schedule and assesses the sequential relationship between tasks. This involves setting one task as the base and comparing its duration or sequence with those of other tasks set as references. Item 2 addresses the specifics regarding work schedules and Excel files. Typically, on-site work schedules are not recorded as separate tasks for each object; instead, each task is noted together with the objects involved. To clarify which

tasks are performed on which objects on the web platform, the work schedule is structured according to Item 2. The work-schedule-file conversion features (Figures A7 and A8) ensure that traditional formats of work schedules yield the same results. Item 3 shows the characteristics extracted from the 3D model elements. Furthermore, the work-schedule data and spatial data of the work objects are double-checked to ensure a comprehensive and accurate representation of the risks (Figure A9). This capability is key to enhancing understanding and awareness of potential hazards on the part of the user, thus facilitating more informed decision-making in risk management.

Table 4. Details regarding application programming interfaces (APIs) for risk-identification algorithm.

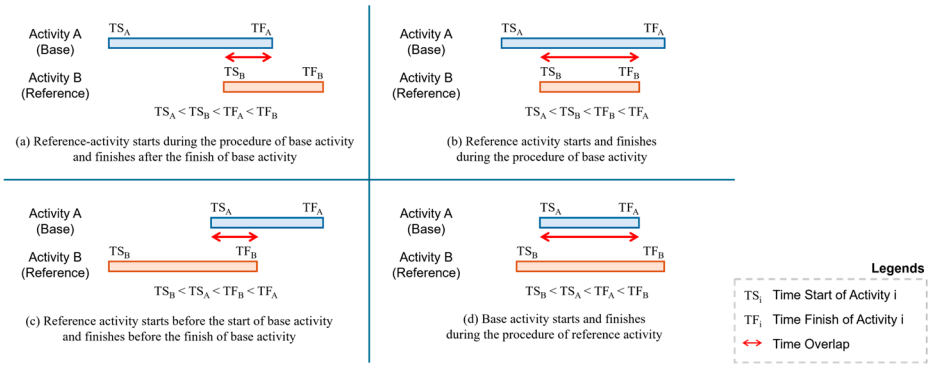

Item 1. Calculation formula for determining job precedence relationship based on work schedule

—	Operation	Detail	CAS No.	Material ID	Work Date	Start Date	2023-04-01	2023-04-02
1.1	Painting	Handling Flammable Material	1110-101	140046	2	2023-04-01		
1.2	Painting	Handling Flammable Material	1110-101	140017	2	2023-04-01		
1.3	Painting	Handling Flammable Material	1110-101	139988	2	2023-04-01		
1.4	Painting	Handling Flammable Material	1110-101	139893	2	2023-04-01		
1.5	Painting	Handling Flammable Material	1110-101	139921	2	2023-04-01		
1.6	Painting	Handling Flammable Material	1110-101	139949	2	2023-04-01		
2.1	Welding	Handling Firearm		144808	1	2023-04-02		
2.2	Welding	Handling Firearm		147051	1	2023-04-02		
2.3	Welding	Handling Firearm		144216	1	2023-04-02		

Item 2. Job schedule (job name, detail, material safety data sheet or MSDS number, unique ID, job date, job start date)
(This is an example of setting the schedule for each task target (the transformation process is omitted))

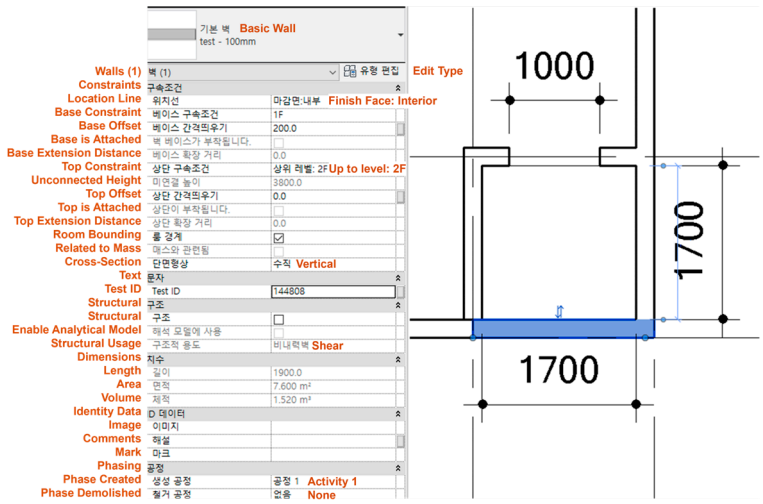

Item 3. Extractive properties example—model element type, constraints, dimensions, etc.

After the uploaded data sources are analyzed based on the embedded features, the analysis results, elucidating the identified risks and corresponding information, are delivered to the users. The prototype system provides visualizations of 3D models, task schedules, and risk-related information through a web-based platform via most web browsers, such as Google Chrome, Microsoft Edge, and Mozilla Firefox (Figure A10). Moreover, all of the data-upload functionalities described earlier can be utilized via the web-based platform.

To further maximize the benefits of BIM for user comprehension, the web-based platform allows for the selection of a risk entity in the 3D model, for which it then provides details about the corresponding risks and basic preventive measures using a pop-up window. This pop-up window, as depicted in Figure 11, includes visual aids such as images of related accident cases or educational resources for risk mitigation by site personnel. It also displays related task schedules, facilitating investigations into the nature of the detected risk. Additionally, to enhance comprehensive understanding on the part of the users and their interaction with the 3D models in a dynamic and informative manner, the web platform supports various views, such as sectional views, floor plans, and 360° rotations, as demonstrated by the rotatable cube in Figure 11 (Figures A5 and A10). Furthermore, users can select specific dates on the web-based platform, enabling them to assess the risks for a chosen day or for a specified period. Our proposed risk-assessment tool facilitates the identification of work objects for which interferences, and consequently risks, can be detected for the selected timeframe (Figure A11).

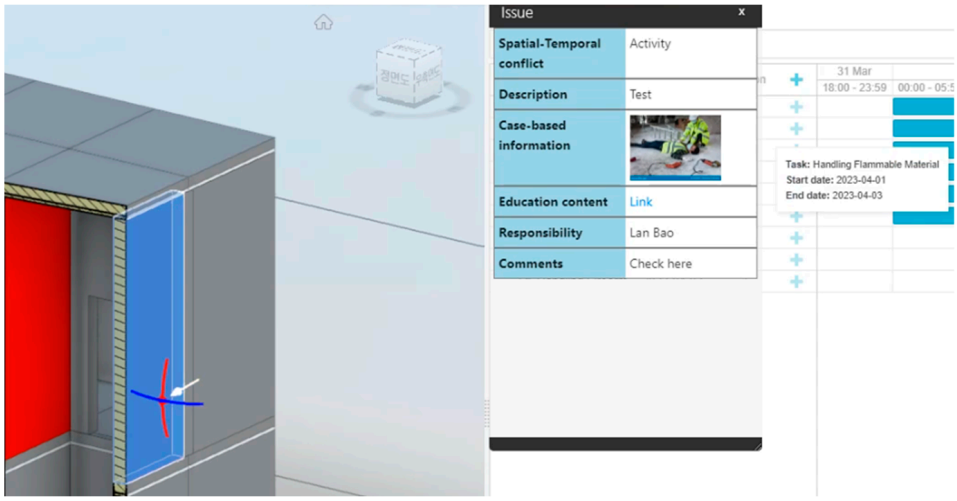

Figure 11. Example of risk-related information pop-up window.

4. Results

To validate the implemented prototype system, we developed basic 3D models in the RTV format, as shown in Figure 12, for testing each scenario. Because the developed risk-identification algorithms target risk factors that do not involve design elements, these models focus solely on spatial data, including only structural components, such as slabs, walls, and openings, that reflect the content of the scenarios.

Figure 13 presents an example that includes a detailed risk-factor identification process and combination formula within the risk-identification framework, specifically focusing on a scenario requiring the detection of fire-related risks.

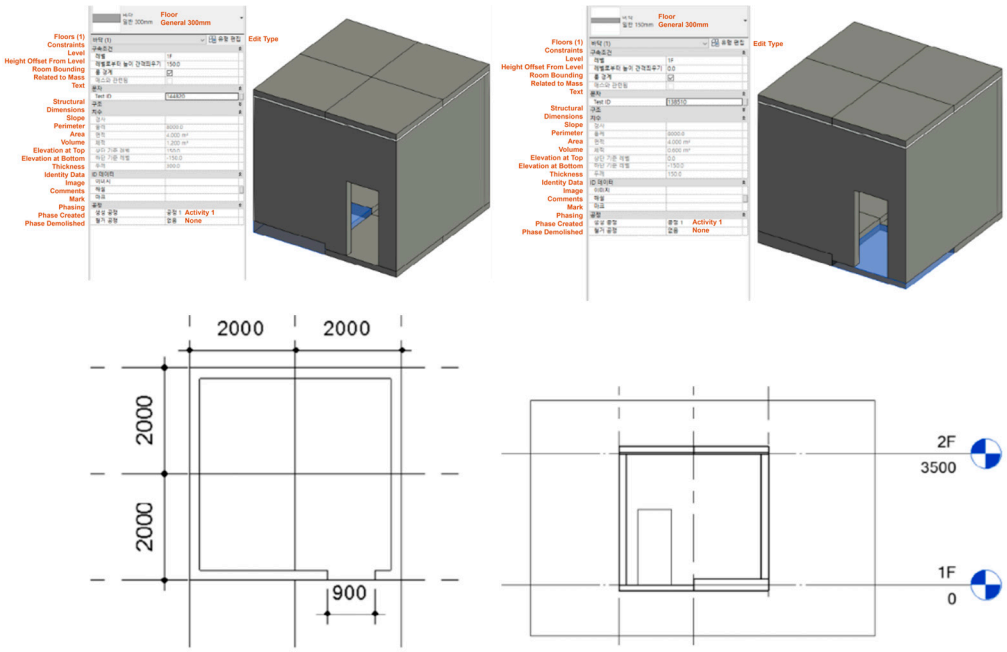

Figure 12. Three-dimensional model with properties for validation.

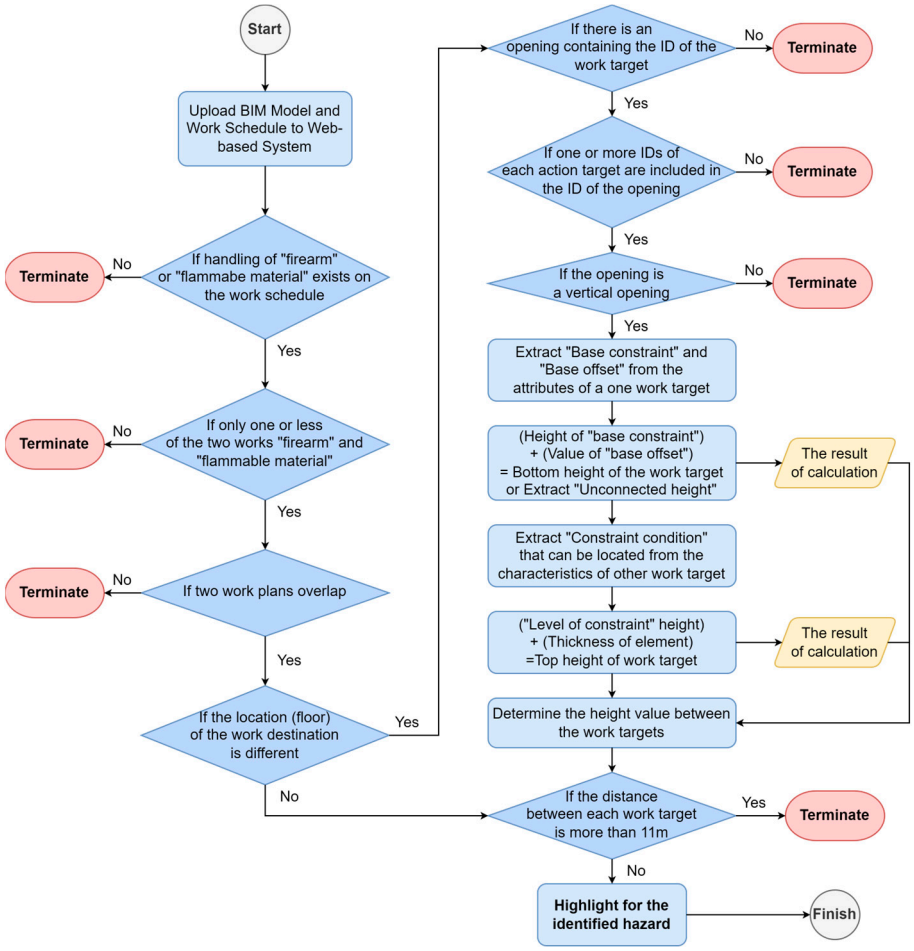

Figure 13. Detailed algorithm configuration for fire-risk identification process.

After the relevant model and work schedule are uploaded, the system first checks for the presence of tasks based on phrases such as "fire-handling" or "flammable-material handling" in the work schedule. If both tasks are detected, it proceeds to determine whether an overlap exists in the task schedules. The subsequent discernment algorithm then extracts properties and geometric data from the BIM model. First, it ascertains the floor on which the target element of each task resides to identify the work location. If the tasks are on different floors, the connectivity of the spaces is determined based on the unique IDs of the openings. Finally, the distances between the task targets are evaluated to assess the potential risk of fire due to flame spread.

For this study, the scenario crafted for testing involved welding tasks and painting using epoxy paint, which were planned to be executed concurrently on different floors but in connected spaces and within a distance of 11 m (36 ft). The algorithms applied, in sequence, were "Task-Target Floor Identification", "Task-Schedule Overlap Detection", "Space Connectivity Detection", and "Task-Target Distance Evaluation".

Figure 14a shows a selected workday with only a painting task scheduled for the basement, resulting in no fire-risk detection. However, in Figure 14b, both painting and welding tasks overlap, prompting a fire-risk alert; the respective task targets are marked in red. This outcome confirms the operational efficiency of the discernment algorithms and risk-identification process.

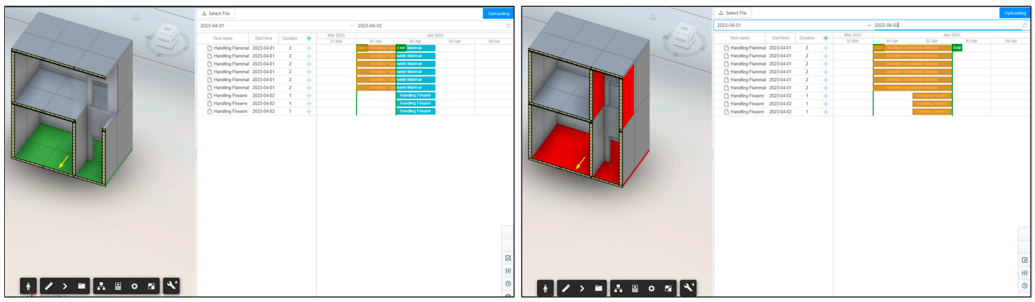

(a) When a painting task is the only task **(b) When both painting and welding tasks overlap**

Figure 14. Validation: fire-risk detection.

Figure 15 illustrates the validation results for a scenario involving fall risks due to pre-tensioned spun high-strength concrete (PHC) piles, where the properties of the material can lead to fall hazards akin to openings. The risk-factor identification algorithms employed were "Material Property Identification" and "Task Sequence Determination". In Figure 15a,b, the selected PHC piles with hollow cylindrical forms pose a fall risk. The internal diameter in Figure 15a is 1600 mm, whereas that in Figure 15b is 1200 mm, both corresponding to a fall hazard. However, in Figure 15c, the pile has an internal diameter of 600 mm, which was determined to be safe and is thus highlighted in green. The final task phase, shown in Figure 15d, involves performing foundational work on top of the pile, sealing the opening, and nullifying the fall risk.

Through validation, we verified the efficiency of the risk-factor identification algorithms and risk-identification process in executing risk discernment. Furthermore, by selecting dates from the work schedule, we confirmed that only the dates with detected risks had their targets shown in red.

In this study, a risk-identification framework that can respond to changes in on-site work conditions due to varying risks is proposed. This framework integrates spatial and temporal data based on 4D BIM. First, a 3D model that requires risk identification and the corresponding work schedule are uploaded to the web platform, where the framework is implemented. A compound algorithm then operates according to the unique risk-identification process of the framework to discern potential risks. Users can select a specific date on the web platform to visually display the work targets where risks have been identified. They can also verify whether these risks change according to the schedule.

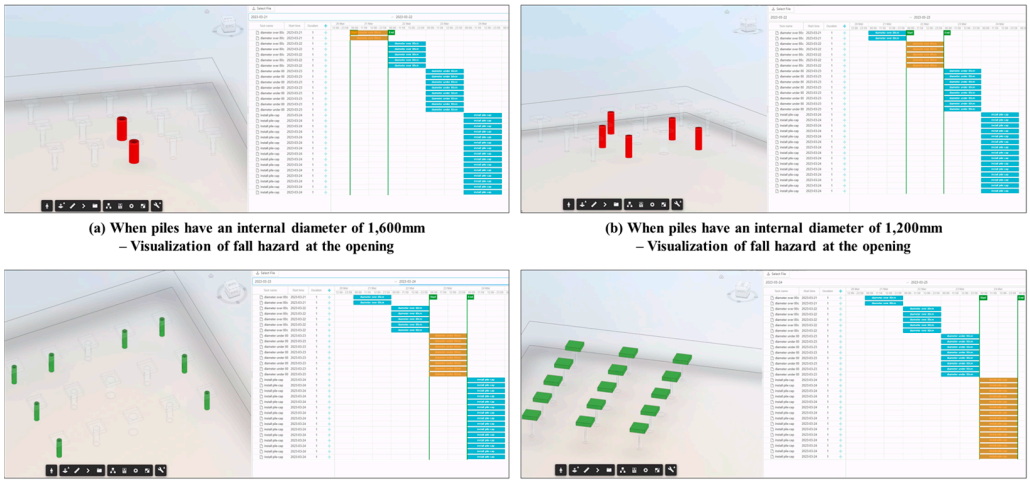

(a) When piles have an internal diameter of 1,600mm – Visualization of fall hazard at the opening

(b) When piles have an internal diameter of 1,200mm – Visualization of fall hazard at the opening

(c) When piles have an internal diameter of 600mm – Visualization of safety from fall hazard at the opening

(d) When the opening is sealed during foundational works on top of the pile – Visualization of safety from fall hazard at the opening

Figure 15. Validation: fall-risk detection.

Figure 14 illustrates the identification of fire-related risks for a scenario in which flammable-material-handling and heat-source-handling tasks occur simultaneously within the same space. The identified risks are highlighted in red. The day-by-day visualization of work targets and their color variations effectively indicate changes in the risk levels. On the other hand, Figure 15 shows how risk levels can change over time, even for the same work target, owing to the progression of construction activities.

In addition, an integration approach based on unique IDs is adopted to connect the 3D model with the work schedule, thereby enabling data acquisition. The web-based platform allows the viewing of the 3D model and work schedule. When a specific date is selected, the 3D model immediately displays the risk-identification results for the selected date.

5. Discussion and Conclusions

This study proposes a novel approach to addressing the problem of information fragmentation in risk assessment by focusing on improving the risk identification phase. Using integrated spatial and temporal data could establish a framework for real-time risk identification based on 4D BIM, and the framework was validated through the implementation of a web-based platform, allowing the capture of risk fluctuations across different scenarios. It is anticipated that this risk-identification framework, which tracks on-site risk factors in real time and visualizes the results on a 3D model, will significantly enhance risk awareness among workers.

The novelty of this research lies in its integration of spatial and temporal data to provide a risk-assessment approach that reflects the real-time dynamics of construction sites. The proposed risk-identification framework tracks changes in risk levels in real time as the actual construction progresses, overcoming the limitations of traditional risk-assessment methods. Furthermore, the identification results are intuitively visualized on a 3D model, effectively conveying the risk information clearly to workers. This study significantly enhanced the accessibility of identified risk information by constructing a web-based platform. Notably, the data from the 3D model and work schedule are interconnected based on unique IDs, successfully facilitating an algorithm that automatically identifies risk factors. In other words, the assessment of safety risks using spatial data within 3D models followed a similar approach to other studies by using pre-defined logics (algorithms), but the novelty of this study is that schedule data are utilized for a more complex assessment of safety risks based on spatial–temporal changes, which sets it apart from other studies.

This approach, which allows users to identify risks simply by uploading a 3D model and work schedule to the system, addresses some of the usability problems inherent in traditional BIM-based tools. Additionally, unlike in the past, wherein a single research

study on risk assessment would be confined to a single type of accident, this study proposes a methodology capable of comprehensive risk identification for multiple types of accidents based on various risk-factor identification algorithms and combination methods. The ability to identify diverse accident types renders this approach more versatile than methods proposed in earlier research studies.

However, despite the findings of this study, several limitations were identified during the research process. First, there is a need for additional information entries in the Excel-based work schedule. Certain details, such as the MSDS number, equipment information, and material data, are necessary and should be included in the Excel file. There have been instances where this information is absent from the work schedule, necessitating its addition. For the risk-identification framework proposed in this study to be usable, it is imperative that this information be accurately entered and updated on-site. Due to this constraint, project managers may be required to exert extra effort and may encounter difficulties during the actual implementation.

Secondly, there is a limitation in the unique-ID-based linkage method used to connect the 3D model with the work schedule. The process of entering the unique ID into the work schedule is separate, and there is a lack of correlation with the serial numbers of the construction components used on-site. To resolve this problem, either harmonization between the unique ID and serial numbers used in the drawings or an automatic unique ID input tool may have to be developed. Consequently, the limitations of this study can be summarized as the need for manual input of some data, and further automation processes should be developed to fully automate the safety risk assessment process.

To further develop and apply BIM- and schedule-based automated safety risk assessment to the actual construction field, the authors propose two future research directions. The first direction is the development of an all-in-one platform that integrates various data sources, such as BIM and construction schedules, utilizing standardized data formats like the Industry Foundation Classes (IFC) standard. Data produced within construction projects are usually established on different platforms and by different stakeholders, and the utilization of different data sources takes extra effort. Besides that, in the study, the authors developed the prototype platform using the Autodesk platform, including Revit. While implemented using the Autodesk Revit model, the platform can be adaptable to open BIM models created with IFC. Other BIM models uploaded to the platform, including their parameters, which follow the algorithm input process, can also be utilized. By utilizing an all-in-one platform and interoperable standards, the application of automated safety risk assessments can be streamlined in a consistent manner. Secondly, real-time data, such as sensor data, can be collected and analyzed for more dynamic risk assessment. The current trend of safety monitoring in construction is the utilization of real-time safety monitoring systems, and integration with various data sources can provide broad insights into assessing site safety risks.

At its core, this study emphasizes the automation of risk identification, adaptable to changes in construction progress, using 4D BIM. It visually represents various risk factors based on assessments using the framework and offers a clear method of communicating risk-identification results. More specifically, safety managers can easily assess the safety risk at their sites using BIM and construction schedule data, and workers can easily understand visualized risks and risk-related information and education links through pop-up windows. More importantly, by structuring scenarios based on actual accident cases and testing them in the system, this study provides concrete guidelines for the comprehensive safety management of construction sites.

Author Contributions: Conceptualization, C.P. and D.L. (Doyeop Lee); methodology, S.V.-T.T., T.Y. and D.L. (Doyeop Lee); software, S.V.-T.T. and T.Y.; validation, S.V.-T.T. and T.Y.; formal analysis, S.V.-T.T., D.K. and T.Y; investigation, D.L. (Doyeop Lee) and T.Y.; resources, C.P. and T.Y.; data curation, D.K.; writing—original draft, T.Y. and D.K.; writing—review and editing, S.V.-T.T., D.L. (Dongmin Lee) and C.P.; visualization, T.Y. and D.K.; supervision, D.L. (Doyeop Lee), D.L. (Dongmin

Lee) and C.P.; project administration, T.Y. and D.K.; funding acquisition, C.P. All authors have read and agreed to the published version of the manuscript.

Funding: This research was conducted with the support of the "National R&D Project for Smart Construction Technology (RS-2020-KA156291)" funded by the Korea Agency for Infrastructure Technology Advancement under the Ministry of Land, Infrastructure and Transport and managed by the Korea Expressway Corporation. This research was supported by the Chung-Ang University Research Scholarship Grants in 2022.

Data Availability Statement: The data that support the findings of this study are available from the corresponding author upon reasonable request.

Conflicts of Interest: The authors declare no conflicts of interest.

Appendix A

```
// POST /api/forge/oss/buckets - creates a new bucket.
// Request body must be a valid JSON in the form of { "bucketKey": "<new_bucket_name>" }.
router.post('/buckets', async (req, res, next) => {
    let payload = new forgeApi.PostBucketsPayload();
    payload.bucketKey = config.credentials.client_id.toLowerCase() + '-' + req.body.bucketKey;
    payload.policyKey = 'persistent'//'transient'; // expires in 24h
    try {
        // Create a bucket using [BucketsApi](https://github.com/Autodesk-Forge/forge-api-nodejs-client/blob/master/docs/BucketsApi.md#createBucket).
        let data = await new forgeApi.BucketsApi().createBucket(payload, {}, req.oauth_client, req.oauth_token)
            .catch(err => {
                res.status(400).end()
            })
        if (data) {
            res.status(200).json({
                id: data.body.bucketKey,
                // Remove bucket key prefix that was added during bucket creation
                text: data.body.bucketKey.replace(config.credentials.client_id.toLowerCase() + '-', ''),
                type: 'bucket',
                icon: "folder-close",
                label: data.body.bucketKey.replace(config.credentials.client_id.toLowerCase() + '-', ''),
                children: true,
                hasCaret: true,
            });
        }

    } catch (err) {
        res.status(400).end()
    }
});

// POST /api/forge/oss/objects - uploads new object to given bucket.
```

Figure A1. Autodesk Forge Bucket code.

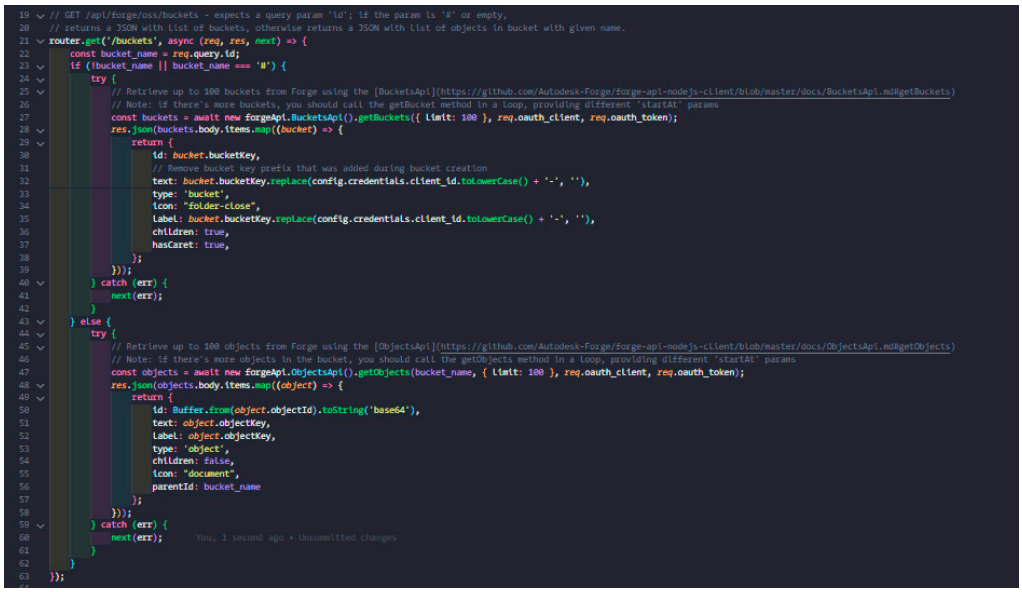

```
// GET /api/forge/oss/buckets - expects a query param 'id'; if the param is '#' or empty,
// returns a JSON with list of buckets, otherwise returns a JSON with list of objects in bucket with given name.
router.get('/buckets', async (req, res, next) => {
    const bucket_name = req.query.id;
    if (!bucket_name || bucket_name === '#') {
        try {
            // Retrieve up to 100 buckets from Forge using the [BucketsApi](https://github.com/Autodesk-Forge/forge-api-nodejs-client/blob/master/docs/BucketsApi.md#getBuckets)
            // Note: if there's more buckets, you should call the getBucket method in a loop, providing different 'startAt' params
            const buckets = await new forgeApi.BucketsApi().getBuckets({ limit: 100 }, req.oauth_client, req.oauth_token);
            res.json(buckets.body.items.map((bucket) => {
                return {
                    id: bucket.bucketKey,
                    // Remove bucket key prefix that was added during bucket creation
                    text: bucket.bucketKey.replace(config.credentials.client_id.toLowerCase() + '-', ''),
                    type: 'bucket',
                    icon: "folder-close",
                    label: bucket.bucketKey.replace(config.credentials.client_id.toLowerCase() + '-', ''),
                    children: true,
                    hasCaret: true,
                };
            }));
        } catch (err) {
            next(err);
        }
    } else {
        try {
            // Retrieve up to 100 objects from Forge using the [ObjectsApi](https://github.com/Autodesk-Forge/forge-api-nodejs-client/blob/master/docs/ObjectsApi.md#getObjects)
            // Note: if there's more objects in the bucket, you should call the getObjects method in a loop, providing different 'startAt' params
            const objects = await new forgeApi.ObjectsApi().getObjects(bucket_name, { limit: 100 }, req.oauth_client, req.oauth_token);
            res.json(objects.body.items.map((object) => {
                return {
                    id: Buffer.from(object.objectId).toString('base64'),
                    text: object.objectKey,
                    label: object.objectKey,
                    type: 'object',
                    children: false,
                    icon: "document",
                    parentId: bucket_name
                };
            }));
        } catch (err) {
            next(err);      You, 1 second ago • Uncommitted changes
        }
    }
});
```

Figure A2. Implementation of API using Autodesk Forge Bucket.

```
// POST /api/forge/oss/objects - uploads new object to given bucket.
// Request body must be structured as 'form-data' dictionary
// with the uploaded file under "fileToUpload" key, and the bucket name under "bucketKey".
router.post('/objects', multer({ dest: 'uploads/' }).single('fileToUpload'), async (req, res, next) => {
    fs.readFile(req.file.path, async (err, data) => {
        if (err) {
            next(err);
        }
        try {
            // Upload an object to bucket using [ObjectsApi](https://github.com/Autodesk-Forge/forge-api-nodejs-client/blob/master/docs/ObjectsApi.md#uploadObject).
            let response = await new forgeApi.ObjectsApi().uploadObject(req.body.bucketKey, req.file.originalname, data.length, data, {}, req.oauth_client, req.oauth_token);
            await fs.unlinkSync(req.file.path)
            if (response) {
                res.status(200).json({
                    id: Buffer.from(response.body.objectId).toString('base64'),
                    text: response.body.objectKey,
                    label: response.body.objectKey,
                    type: 'object',
                    children: false,
                    icon: "document",
                    parentId: req.body.bucketKey
                });
            } else {
                res.status(400).end();
            }

        } catch (err) {
            await fs.unlinkSync(req.file.path)
            res.status(400).end();
        }
    });
});
```

Figure A3. RVT file upload code.

```
// POST /api/forge/modelderivative/jobs - submits a new translation job for given object URN.
// Request body must be a valid JSON in the form of { "objectName": "<translated-object-urn>" }.
router.post('/jobs', async (req, res, next) => {
  let job = new forgeApi.JobPayload();
  job.input = new forgeApi.JobPayloadInput();
  job.input.urn = req.body.objectName;
  job.output = new forgeApi.JobPayloadOutput([
    new forgeApi.JobSvfOutputPayload()
  ]);
  job.output.formats[0].type = 'svf';
  job.output.formats[0].views = ['2d', '3d'];
  try {
    // Submit a translation job using [DerivativesApi](https://github.com/Autodesk-Forge/forge-api-nodejs-client/blob/master/docs/DerivativesApi.md#translate).
    await new forgeApi.DerivativesApi().translate(job, { xAdsForce: true }, req.oauth_client, req.oauth_token);
    res.status(200).end();
    let progress = 0;
    var manifest = ''
    do {
      manifest = await new forgeApi.DerivativesApi().getManifest(req.body.objectName, {}, req.oauth_client, req.oauth_token);
      var reg = manifest.body.progress.split("%")
      progress = isNumber(reg[0]) ? parseInt(reg[0]) : 100;
      console.log('> ', progress)
    }
    while (progress < 100);
  } catch (err) {
    // next(err);
    res.status(400).end(err);
  }
});
function isNumber(input) {
}
```

Figure A4. Conversion of RVT files into web 3D models.

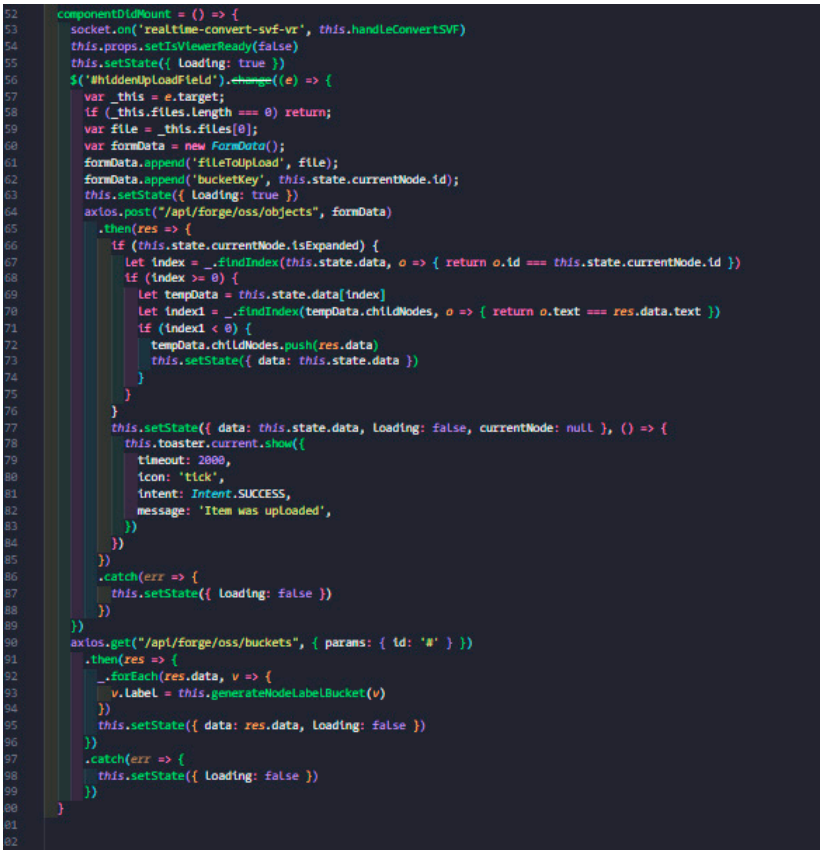

```
componentDidMount = () => {
  socket.on('realtime-convert-svf-vr', this.handleConvertSVF)
  this.props.setIsViewerReady(false)
  this.setState({ loading: true })
  $('#hiddenUploadFileId').change((e) => {
    var _this = e.target;
    if (_this.files.length === 0) return;
    var file = _this.files[0];
    var formData = new FormData();
    formData.append('fileToUpload', file);
    formData.append('bucketKey', this.state.currentNode.id);
    this.setState({ loading: true })
    axios.post("/api/forge/oss/objects", formData)
      .then(res => {
        if (this.state.currentNode.isExpanded) {
          let index = _.findIndex(this.state.data, o => { return o.id === this.state.currentNode.id })
          if (index >= 0) {
            let tempData = this.state.data[index]
            let index1 = _.findIndex(tempData.childNodes, o => { return o.text === res.data.text })
            if (index1 < 0) {
              tempData.childNodes.push(res.data)
              this.setState({ data: this.state.data })
            }
          }
        }
        this.setState({ data: this.state.data, loading: false, currentNode: null }, () => {
          this.toaster.current.show({
            timeout: 2000,
            icon: 'tick',
            intent: Intent.SUCCESS,
            message: 'Item was uploaded',
          })
        })
      })
      .catch(err => {
        this.setState({ loading: false })
      })
  })
  axios.get("/api/forge/oss/buckets", { params: { id: '#' } })
    .then(res => {
      _.forEach(res.data, v => {
        v.label = this.generateNodeLabelBucket(v)
      })
      this.setState({ data: res.data, loading: false })
    })
    .catch(err => {
      this.setState({ loading: false })
    })
}
```

Figure A5. Upload and use of 3D models on web platform.

```
const handleLoadGant = async () => {
  groupEl = await getProperty()
  gantt.importFromExcel({
    server: "https://export.dhtmlx.com/gantt",
    data: file,
    callback: function (project) {
      if (project) {
        gantt.clearAll();
        markers = []
        var mapping = {
          '#': "wbs",
          'Duration'
            :
            "duration",
          'Start time'
            :
            "start_date",
          'Task name'
            :
            "text"
        }
        var ganttDataset = {
          data: [],
          links: []
        };

        project.forEach(function (item) {
          var copy = {};
          for (var i in item) {
            if (mapping[i]) {
              copy[mapping[i]] = item[i];
            } else {
              copy[to_snake_case(i)] = item[i];
            }

            copy.open = true;
            if (copy.wbs) {
              var wbs = copy.wbs + "";
              copy.id = wbs;
              var parts = wbs.split(".");
              parts.pop();
              copy.parent = parts.join(".");
            }
          }
          ganttDataset.data.push(copy);
        });

        gantt.parse(ganttDataset);
        markers.push(gantt.addMarker({
          start_date: area[0].toDate(),
          css: "start-timeline",
          text: "Start",

        }))
        markers.push(gantt.addMarker({
          start_date: area[1].toDate(),
          css: "end-timeline",
          text: "End",

        }))
        handleRangePicker(area)
      }
    }
  });

}
```

Figure A6. Acquisition of data from Excel file.

```
useEffect(() => {
  if (ref.current) {
    gantt.config.row_height = 24;
    gantt.plugins({
      fullscreen: true,
      drag_timeline: true,
      auto_scheduling: true,
      undo: true,
      tooltip: true,
      marker: true,
      critical_path: true,
      grouping: true
    });
    var zoomConfig = {
      levels: [
        [
          { unit: "month", format: "%M %Y", step: 1 },
          {
            unit: "week", step: 1, format: function (date) {
              var dateToStr = gantt.date.date_to_str("%d %M");
              var endDate = gantt.date.add(date, -6, "day");
              var weekNum = gantt.date.date_to_str("%W")(date);
              return "Week #" + weekNum + ", " + dateToStr(date) + " - " + dateToStr(endDate);
            }
          }
        ],
        [
          { unit: "month", format: "%M %Y", step: 1 },
          { unit: "day", format: "%d %M", step: 1 }
        ],
        [
          { unit: "day", format: "%d %M", step: 1 },
          { unit: "hour", format: hourRangeFormat(12), step: 12 }
        ],
        [
          { unit: "day", format: "%d %M", step: 1 },
          { unit: "hour", format: hourRangeFormat(6), step: 6 }
        ],
        [
          { unit: "day", format: "%d %M", step: 1 },
          { unit: "hour", format: "%H:%i", step: 1 }
        ]
      ],
      useKey: "ctrlKey",
      trigger: "wheel",
      element: function () {
        return gantt.$root.querySelector(".gantt_task");
      }
    };
    gantt.ext.zoom.init(zoomConfig);
    gantt.init(ref.current);
    events.push(gantt.attachEvent("onTaskClick", (id, e) => {
      if (window.viewer) {
        let task = gantt.getTask(id)
        console.log(task)
        window.viewer.search(task.id, onSuccessCallback, onErrorCallback, ['properties', 'Task ID', 'Activity ID'])
      }

    }))
  }
}, [ref.current])
```

Figure A7. Upload and initiation of task schedule.

```
return (
  <>
    <div style={{ display: 'flex', flexDirection: 'column', gap: 5 }}>
      <div style={{ display: 'flex', flexWrap: 'wrap', justifyContent: 'space-between' }}  >
        <Upload
          customRequest={handleChangeModel}
          showUploadList={false}
        >
          <Button icon={<UploadOutlined />}>Select File</Button>
        </Upload>
        <Button
          type="primary"
          onClick={handleLoadGant}
          disabled={!file}

        >
          {true ? 'Uploading' : 'Start Upload'}
        </Button>
      </div>
      <div style={{ width: '100%' }}>
        <DatePicker.RangePicker style={{ width: '100%' }} onChange={handleRangePicker} value={area} />
      </div>
    </div>

    <div style={{ height: '100%' }} >
      <div style={{ height: '100%', width: "100%" }}
        ref={ref}

      ></div>
    </div>

    {isOpen && <TestPopup isOpen={isOpen} close={setIsOpen} />}
  </>
```

Figure A8. Conversion of work schedule for use within the web platform.

```
const hightlightArea = (time) => {
  if (taskLayerId) {
    gantt.removeTaskLayer(taskLayerId)
  }
  taskLayerId = gantt.addTaskLayer(function (task) {
    if (task.start_date > time[0] || task.end_date > time[0]) {
      var start_date = time[0];
      var end_date = time[1];
      if (task.start_date > time[0]) start_date = task.start_date;
      if (task.end_date < time[1]) end_date = task.end_date;
      var sizes = gantt.getTaskPosition(task, start_date, end_date);
      var el = document.createElement('div');
      el.className = 'progress_value';
      el.style.left = sizes.left + 'px';
      el.style.width = sizes.width + 'px';
      el.style.top = sizes.top + 2 + 'px';
      el.style.height = sizes.height + 'px';
      return el;
    }
    return false;
  });
}
```

Figure A9. Task-target highlights.

```
handleOpenViewer = (node) => {
  if (node.type === 'object') {
    this.setState({ loading: true })
    var urn = node.id;
    getForgeToken(token => {
      axios.get('https://developer.api.autodesk.com/modelderivative/v2/designdata/' + urn + '/manifest', {
        headers: {
          'Authorization': `Bearer ${token}`,
        }
      })
        .then(res => {
          this.setState({ loading: false })
          if (res.data.status === 'success') {

            this.setState({ currentNode: node, currentUrn: urn }, () => {
              // this.LaunchViewer(urn);
            })
          }
          else {
            this.toaster.current.show({
              timeout: 2000,
              icon: 'swap-horizontal',
              intent: Intent.NONE,
              message: 'The translation job still running: ' + res.data.progress + '. PLease try again in a moment.',
            }, "progress")
          }
        })
        .catch(err => {
          this.setState({ loading: false })
          this.toaster.current.show({
            timeout: 0,
            icon: 'warning-sign',
            action: {
              onClick: () => {
                axios.post("/api/forge/modelderivative/jobs", { 'bucketKey': node.parentId, 'objectName': node.id })
                  .then(res => {
                    this.toaster.current.dismiss('translate')
                    this.toaster.current.show({
                      timeout: 2000,
                      icon: 'swap-horizontal',
                      intent: Intent.NONE,
                      message: 'Starting translation',
                    }, "progress")
                  })
                  .catch(err => {
                    this.setState({ loading: false })
                  })
              },
              text: <strong>Translate</strong>,
            },
            intent: Intent.WARNING,
            message: 'This file is not translated yet!',
          }, "translate")
        })
    })

  }
}
handleTranslateItem = (e) => {
```

Figure A10. 3D model viewer features.

```
const handleRangePicker = (e) => {
  setArea(e)
  let time = [e[0].toDate(), e[1].toDate()]
  gantt.getMarker(markers[0]).start_date = time[0]
  gantt.getMarker(markers[1]).start_date = time[1]
  gantt.renderMarkers()
  hightLightArea(time)
  let check = 0
  let tempCheck = []
  window.viewer.clearThemingColors()
  gantt.eachTask(task => {
    let children = gantt.getChildren(task.id)
    if (children.length === 0) {
      let start = moment(task.start_date)
      let end = moment(task.end_date)
      if (start >= e[1]) {
        if (groupEl[task.id]) {
          _.forEach(groupEl[task.id], v => {
            window.viewer.hide(v, window.viewer.impl.model)
          })

        }


      } else if (end <= e[0]) {
        if (groupEl[task.id]) {
          _.forEach(groupEl[task.id], v => {
            window.viewer.hide(v, window.viewer.impl.model)
          })

        }
      } else {
        if (groupEl[task.id]) {
          check++
          _.forEach(groupEl[task.id], v => {
            window.viewer.show(v, window.viewer.impl.model)
            window.viewer.setThemingColor(v, convertHexColorToVector4('#6AA84F'), window.viewer.impl.model, true)
            tempCheck.push(v)
          })


        }
      }
    }
  })
  if (check > 1)
    _.forEach(tempCheck, v => {
      window.viewer.setThemingColor(v, convertHexColorToVector4('#CC0000'), window.viewer.impl.model, true)
    })
  gantt.render();
}
```

Figure A11. Selection of start and end dates within work schedule.

References

1. Dewlaney, K.S.; Hallowell, M.R.; Fortunato, B.R. Safety Risk Quantification for High Performance Sustainable Building Construction. *J. Constr. Eng. Manag.* **2012**, *138*, 964–971. [CrossRef]
2. Go, H.; Hyun, J.; Lee, J.; Ahn, J. Development of A Quantitative Risk Assessment Model by BIM-based Risk Factor Extraction—Focusing on Falling Accidents. *Korean J. Constr. Eng. Manag.* **2022**, *23*, 15–25. [CrossRef]
3. Jung, Y.; Kang, S.; Kim, Y.S.; Park, C. Assessment of safety management information systems for general contractors. *Saf. Sci.* **2008**, *46*, 661–674. [CrossRef]
4. Zou, Y.; Kiviniemi, A.; Jones, S.W. A review of risk management through BIM and BIM-related technologies. *Saf. Sci.* **2017**, *97*, 88–98. [CrossRef]
5. Bae, S.; Cha, H. A Method on Developing 3D/BIM-Based Real Time Fire Disaster Information Management. *Korean J. Constr. Eng. Manag.* **2023**, *24*, 3–12. [CrossRef]
6. Tixier, A.J.P.; Hallowell, M.R.; Rajagopalan, B.; Bowman, D. Construction Safety Clash Detection: Identifying Safety Incompatibilities among Fundamental Attributes using Data Mining. *Autom. Constr.* **2017**, *74*, 39–54. [CrossRef]
7. Hongling, G.; Yantao, Y.; Weisheng, Z.; Yan, L. BIM and Safety Rules Based Automated Identification of Unsafe Design Factors in Construction. *Procedia Eng.* **2016**, *164*, 467–472. [CrossRef]
8. Tran, S.V.T.; Khan, N.; Lee, D.; Park, C. A hazard identification approach of integrating 4d bim and accident case analysis of spatial–temporal exposure. *Sustainability* **2021**, *13*, 2211. [CrossRef]
9. Kiviniemi, M.; Sulankivi, K.; Kähkönen, K.; Mäkelä, T.; Merivirta, M.-L. BIM-Based Safety Management and Communication for Building Construction. VTT Research Notes 2597. 2011. Available online: https://publications.vtt.fi/pdf/tiedotteet/2011/T2597.pdf (accessed on 31 May 2024).
10. Zhang, S.; Sulankivi, K.; Kiviniemi, M.; Romo, I.; Eastman, C.M.; Teizer, J. BIM-based fall hazard identification and prevention in construction safety planning. *Saf. Sci.* **2015**, *72*, 31–45. [CrossRef]
11. Kim, I.; Lee, Y.; Choi, J. BIM-based hazard recognition and evaluation methodology for automating construction site risk assessment. *Appl. Sci.* **2020**, *10*, 2335. [CrossRef]
12. Benjaoran, V.; Bhokha, S. An integrated safety management with construction management using 4D CAD model. *Saf. Sci.* **2010**, *48*, 395–403. [CrossRef]

13. Zhang, S.; Teizer, J.; Lee, J.K.; Eastman, C.M.; Venugopal, M. Building Information Modeling (BIM) and Safety: Automatic Safety Checking of Construction Models and Schedules. *Autom. Constr.* **2013**, *29*, 183–195. [CrossRef]
14. Crowther, J.; Ajayi, S.O. Impacts of 4D BIM on construction project performance. *Int. J. Constr. Manag.* **2021**, *21*, 724–737. [CrossRef]
15. Eastman, C.; Teicholz, P.; Sacks, R.; Liston, K. BIM for Architects and Engineers. In *BIM Handbook: A Guide to Building Information Modeling for Owners, Managers, Designers, Engineers, and Contractors*, 2nd ed.; John Wiley & Sons, Inc.: Hoboken, NJ, USA, 2011; pp. 149–204.
16. Pinto, A.; Nunes, I.L.; Ribeiro, R.A. Occupational risk assessment in construction industry—Overview and reflection. *Saf. Sci.* **2011**, *49*, 616–624. [CrossRef]
17. Harms-Ringdahl, L. Relationships between accident investigations, risk analysis, and safety management. *J. Hazard. Mater.* **2004**, *111*, 13–19. [CrossRef] [PubMed]
18. *ISO 310002018*; ISO 31000:2018 Risk Management—Guidelines. ISO—The International Organization for Standardization: Geneva, Switzerland, 2018.
19. *IEC 310102019*; IEC 31010:2019 Risk Management—Risk Assessment Techniques. ISO—International Organization for Standardization: Geneva, Switzerland, 2019.
20. Rouvroye, J.L.; Van Den Bliek, E.G. Comparing safety analysis techniques. *Reliab. Eng. Syst. Saf.* **2002**, *75*, 289–294. [CrossRef]
21. Navon, R.; Asce, M.; Kolton, O. Model for Automated Monitoring of Fall Hazards in Building Construction. *J. Constr. Eng. Manag.* **2006**, *132*, 733–740. [CrossRef]
22. Jou, Y.T.; Lin, C.J.; Yenn, T.C.; Yang, C.W.; Yang, L.C.; Tsai, R.C. The implementation of a human factors engineering checklist for human-system interfaces upgrade in nuclear power plants. *Saf. Sci.* **2009**, *47*, 1016–1025. [CrossRef]
23. Gürcanli, G.E.; Müngen, U. An occupational safety risk analysis method at construction sites using fuzzy sets. *Int. J. Ind. Ergon.* **2009**, *39*, 371–387. [CrossRef]
24. Wu, W.; Gibb, A.G.F.; Li, Q. Accident precursors and near misses on construction sites: An investigative tool to derive information from accident databases. *Saf. Sci.* **2010**, *48*, 845–858. [CrossRef]
25. Aneziris, O.N.; Papazoglou, I.A.; Kallianiotis, D. Occupational risk of tunneling construction. *Saf. Sci.* **2010**, *48*, 964–972. [CrossRef]
26. Kim, K.; Lee, Y.C. Automated generation of daily evacuation paths in 4D BIM. *Appl. Sci.* **2019**, *9*, 1789. [CrossRef]
27. Tran, S.V.T.; Nguyen, T.L.; Chi, H.L.; Lee, D.; Park, C. Generative planning for construction safety surveillance camera installation in 4D BIM environment. *Autom. Constr.* **2022**, *134*, 104103. [CrossRef]
28. Mirzaei, A.; Nasirzadeh, F.; Parchami Jalal, M.; Zamani, Y. 4D-BIM Dynamic Time–Space Conflict Detection and Quantification System for Building Construction Projects. *J. Constr. Eng. Manag.* **2018**, *144*, 04018056. [CrossRef]
29. Shim, C.S.; Lee, K.M.; Kang, L.S.; Hwang, J.; Kim, Y. Three-dimensional information model-based bridge engineering in Korea. *Struct. Eng. Int.* **2012**, *22*, 8–13. [CrossRef]
30. Arslan, M.; Cruz, C.; Ginhac, D. Visualizing intrusions in dynamic building environments for worker safety. *Saf. Sci.* **2019**, *120*, 428–446. [CrossRef]
31. Fargnoli, M.; Lombardi, M. Building information modelling (BIM) to enhance occupational safety in construction activities: Research trends emerging from one decade of studies. *Buildings* **2020**, *10*, 98. [CrossRef]
32. Qi, J.; Issa, R.R.A.; Hinze, J.; Olbina, S. Integration Of Safety In Design Through The Use Of Building Information Modeling. In Proceedings of the Computing in Civil Engineering, Miami, FL, USA, 19 June 2011. [CrossRef]
33. Ho, S.P.; Tserng, H.P.; Jan, S.H. Enhancing knowledge sharing management using BIM technology in construction. *Sci. World J.* **2013**, *2013*, 170498. [CrossRef] [PubMed]
34. Nizam, R.S.; Zhang, C.; Tian, L. A BIM based tool for assessing embodied energy for buildings. *Energy Build.* **2018**, *170*, 1–14. [CrossRef]
35. Yuan, J.; Li, X.; Xiahou, X.; Tymvios, N.; Zhou, Z.; Li, Q. Accident prevention through design (PtD): Integration of building information modeling and PtD knowledge base. *Autom. Constr.* **2019**, *102*, 86–104. [CrossRef]
36. Hardison, D.; Hallowell, M. Construction hazard prevention through design: Review of perspectives, evidence, and future objective research agenda. *Saf. Sci.* **2019**, *120*, 517–526. [CrossRef]
37. Swallow, M.; Zulu, S. Benefits and barriers to the adoption of 4d modeling for site health and safety management. *Front. Built Environ.* **2019**, *4*, 86. [CrossRef]
38. Lu, Y.; Gong, P.; Tang, Y.; Sun, S.; Li, Q. BIM-integrated construction safety risk assessment at the design stage of building projects. *Autom. Constr.* **2021**, *124*, 103553. [CrossRef]
39. Chien, K.F.; Wu, Z.H.; Huang, S.C. Identifying and assessing critical risk factors for BIM projects: Empirical study. *Autom. Constr.* **2014**, *45*, 1–15. [CrossRef]
40. Jin, Z.; Gambatese, J.; Liu, D.; Dharmapalan, V. Using 4D BIM to assess construction risks during the design phase. *Eng. Constr. Archit. Manag.* **2019**, *26*, 2637–2654. [CrossRef]
41. Tixier, J.; Dusserre, G.; Salvi, O.; Gaston, D. Review of 62 risk analysis methodologies of industrial plants. *J. Loss Prev. Process Ind.* **2002**, *15*, 291–303. [CrossRef]
42. Andriessen, J.H.T.H. Safe Behaviour and Safety Motivation. *J. Occup. Accid.* **1978**, *1*, 363–376. [CrossRef]

43. Li, S.; Wu, X.; Wang, X.; Hu, S. Relationship between Social Capital, Safety Competency, and Safety Behaviors of Construction Workers. *J. Constr. Eng. Manag.* **2020**, *146*, 04020059. [CrossRef]
44. Meng, Q.; Liu, W.; Li, Z.; Hu, X. Influencing factors, mechanism and prevention of construction workers' unsafe behaviors: A systematic literature review. *Int. J. Environ. Res. Public Health* **2021**, *18*, 2644. [CrossRef]
45. Zid, C.; Kasim, N.; Benseghir, H.; Nomani Kabir, M.; Bin Ibrahim, A. Developing an Effective Conceptual Framework for Safety Behaviour in Construction Industry. *E3S Web Conf.* **2018**, *65*, 03006. [CrossRef]
46. Yang, Y.K.; Kim, B.S. Study on the Structural Relation between the Level of Fatigue and Stress of Construction Workers and Disaster Risks. *J. Korea Saf. Manag. Sci.* **2014**, *16*, 35–44. [CrossRef]
47. Wang, D.; Wang, X.; Xia, N. How safety-related stress affects workers' safety behavior: The moderating role of psychological capital. *Saf. Sci.* **2018**, *103*, 247–259. [CrossRef]
48. Chen, Y.; Li, S. Relationship Between Workplace Ostracism and Unsafe Behaviors: The Mediating Effect of Psychological Detachment and Emotional Exhaustion. *Psychol. Rep.* **2020**, *123*, 488–516. [CrossRef]
49. Wu, X.; Li, Y.; Yao, Y.; Luo, X.; He, X.; Yin, W. Development of construction workers job stress scale to study and the relationship between job stress and safety behavior: An empirical study in Beijing. *Int. J. Environ. Res. Public Health* **2018**, *15*, 2409. [CrossRef]
50. Kim, G.-H. The Survey of Construction Workers' Preference for Introducing the Emotional Safety in School Facility Construction-Focused on Emotional Safety Sensor and Emotional Facilities. *J. Sustain. Des. Educ. Environ. Res.* **2011**, *10*, 26–33. [CrossRef]
51. Fang, D.; Jiang, Z.; Zhang, M.; Wang, H. An experimental method to study the effect of fatigue on construction workers' safety performance. *Saf. Sci.* **2015**, *73*, 80–91. [CrossRef]
52. Sing, C.P.; Asce, M.; Love, P.E.D.; Fung, I.W.H.; Edwards, D.J. Personality and Occupational Accidents: Bar Benders in Guangdong Province, Shenzhen, China. *J. Constr. Eng. Manag.* **2014**, *140*, 05014005. [CrossRef]
53. Hasanzadeh, S.; Esmaeili, B.; Dodd, M.D. Examining the Relationship between Personality Characteristics and Worker's Attention under Fall and Tripping Hazard Conditions. In Proceedings of the Construction Research Congress 2018, New Orleans, LA, USA, 2 April 2018. [CrossRef]
54. Al-Bayati, A.J.; Abudayyeh, O.; Fredericks, T.; Butt, S.E. Managing Cultural Diversity at U.S. Construction Sites: Hispanic Workers' Perspectives. *J. Constr. Eng. Manag.* **2017**, 04017064. [CrossRef]
55. Al-Bayati, A.J.; Asce, M. Satisfying the Need for Diversity Training for Hispanic Construction Workers and Their Supervisors at US Construction Workplaces: A Case Study. *J. Constr. Eng. Manag.* **2019**, *145*, 05019007. [CrossRef]
56. Zohar, D. Safety climate in industrial organizations: Theoretical and applied implications. *J. Appl. Psychol.* **1980**, *65*, 96–102. [CrossRef]
57. Arcury, T.A.; Mills, T.; Marín, A.J.; Summers, P.; Quandt, S.A.; Rushing, J.; Lang, W.; Grzywacz, J.G. Work safety climate and safety practices among immigrant Latino residential construction workers. *Am. J. Ind. Med.* **2012**, *55*, 736–745. [CrossRef] [PubMed]
58. Fang, D.; Wu, C.; Wu, H. Impact of the Supervisor on Worker Safety Behavior in Construction Projects. *J. Manag. Eng.* **2015**, *31*, 04015001. [CrossRef]
59. Shen, Y.; Ju, C.; Koh, T.Y.; Rowlinson, S.; Bridge, A.J. The impact of transformational leadership on safety climate and individual safety behavior on construction sites. *Int. J. Environ. Res. Public Health* **2017**, *14*, 45. [CrossRef]
60. Xiong, C.; Liang, K.; Luo, H.; Fung, I.W.H. Identification of safety-related opinion leaders among construction workers: Evidence from scaffolders of metro construction in Wuhan, China. *Int. J. Environ. Res. Public Health* **2018**, *15*, 2176. [CrossRef] [PubMed]
61. Yue, H.; Lianbo, Z. A Study of the Effect of Safety Education for Construction Personnel Based on Human Factors Engineering. *Ind. Eng. J.* **2016**, *19*, 89–94.
62. Du, J.; Wang, J.; Ning, D.; Wang, W. Priority Analysis of Management Method for the Workers' Unsafe Behaviors on Mine Construction Project. In Proceedings of the International Conference on Internet Technology and Applications (iTAP), Wuhan, China, 1–4 August 2010. [CrossRef]
63. Kim, D.K.; Park, S. Business Cycle and Occupational Accidents in Korea. *Saf. Health Work* **2020**, *11*, 314–321. [CrossRef] [PubMed]
64. Iyer, P.S.; Haight, J.M.; Del Castillo, E.; Tink, B.W.; Hawkins, P.W. Intervention effectiveness research: Understanding and optimizing industrial safety programs using leading indicators. *Chem. Health Saf.* **2004**, *11*, 9–19. [CrossRef]
65. Mohamed, S. Safety Climate in Construction Site Environments. *J. Constr. Eng. Manag.* **2002**, *128*, 367–462. [CrossRef]
66. Johnson, H.M.; Singh, A.; Young, R.H.F. Fall Protection Analysis for Workers on Residential Roofs. *J. Constr. Eng. Manag.* **1998**, *124*, 343–433. [CrossRef]
67. Kaskutas, V.; Dale, A.M.; Lipscomb, H.; Gaal, J.; Fuchs, M.; Evanoff, B. Fall prevention among apprentice carpenters. *Scand. J. Work Environ. Health* **2010**, *36*, 258–265. [CrossRef]
68. Chi, S.; Han, S.; Kim, D.Y. Relationship between Unsafe Working Conditions and Workers' Behavior and Impact of Working Conditions on Injury Severity in U.S. Construction Industry. *J. Constr. Eng. Manag.* **2013**, *139*, 826–838. [CrossRef]
69. Zhao, D.; Thabet, W.; McCoy, A.; Kleiner, B. Electrical deaths in the US construction: An analysis of fatality investigations. *Int. J. Inj. Contr. Saf. Promot.* **2014**, *21*, 278–288. [CrossRef] [PubMed]
70. Li, H.; Li, X.; Luo, X.; Siebert, J. Investigation of the causality patterns of non-helmet use behavior of construction workers. *Autom. Constr.* **2017**, *80*, 95–103. [CrossRef]
71. Bureau of Labor Statistics. *Construction Deaths Due to Falls, Slips, and Trips Increased 5.9 Percent in 2021*; US Department of Labor, Bureau of Labor Statistics: Washington, DC, USA, 2023. Available online: https://www.bls.gov/opub/ted/2023/construction-deaths-due-to-falls-slips-and-trips-increased-5-9-percent-in-2021.htm (accessed on 3 June 2024).

72. Harris, W.; Yohannes, T.; Trueblood, A.B. *Fatal and Nonfatal Focus Four Injuries in Construction*; The Center for Construction Research and Training (CPWR): Silver Spring, MD, USA, 2023.
73. The Center for Construction Research and Training (CPWR). *Fatal and Nonfatal Injuries in Construction*; The Center for Construction Research and Training (CPWR): Silver Spring, MD, USA, 2023. Available online: https://www.cpwr.com/research/data-center/data-dashboards/fatal-and-nonfatal-injuries-in-construction/ (accessed on 3 June 2024).
74. Brown, S.; Harris, W.; Brooks, R.D.; Sue Dong, X. *Fatal and Nonfatal Struck-by Injuries in the Construction Industry, 2011–2019*; Centers for Disease Control and Prevention (CDC): Atlanta, GA, USA, 2021. Available online: https://wwwn.cdc.gov/wisards/oiics/ (accessed on 3 June 2024).
75. Bureau of Labor Statistics. *Fatal Occupational Injuries by Industry and Event or Exposure, All United States, 2020*; US Department of Labor, Bureau of Labor Statistics: Washington, DC, USA, 2021. Available online: https://www.bls.gov/iif/fatal-injuries-tables/fatal-occupational-injuries-table-a-1-2020.htm (accessed on 3 June 2024).
76. The Center for Construction Research and Training (CPWR). *Musculoskeletal Disorders (MSDs) in Construction*; The Center for Construction Research and Training (CPWR): Silver Spring, MD, USA, 2023. Available online: https://www.cpwr.com/research/data-center/data-dashboards/musculoskeletal-disorders-in-construction/ (accessed on 3 June 2024).